applied sciences

MDPI

Review

Advancements in Copper-Based Catalysts for Efficient Generation of Reactive Oxygen Species from Peroxymonosulfate

Bakhta Bouzayani [1,2], Bárbara Lomba-Fernández [1], Antía Fdez-Sanromán [1], Sourour Chaâbane Elaoud [2] and Maria Ángeles Sanromán [1,*]

[1] CINTECX, Department of Chemical Engineering, University of Vigo, Campus As Lagoas-Marcosende, 36310 Vigo, Spain; bbouzayanibakhta@gmail.com (B.B.); barbara.lomba.fernandez@uvigo.gal (B.L.-F.); antia.fernandez.sanroman@uvigo.gal (A.F.-S.)

[2] Laboratory of Physical Chemistry of the Solid State, Department of Chemical, University of Sfax, Sfax 3000, Tunisia; sourourelaoud@yahoo.com

* Correspondence: sanroman@uvigo.es

Abstract: Over the past few decades, peroxymonosulfate (PMS)-driven advanced oxidation processes (AOPs) have garnered substantial interest in the field of organic decontamination. The copper (Cu)/PMS system is intriguing due to its diverse activation pathways and has been extensively employed for the clearance of refractory organic pollutants in water. This article is designed to offer a comprehensive overview of the latest trends in Cu-based catalysts such as single-metal and mixed-metal catalysts aimed at treating recalcitrant pollutants, highlighting PMS activation. Subsequently, investigative methodologies for assessing PMS activation with copper-based catalysts are reviewed and summarized. Then, the implications of pH, PMS and catalytic agent concentrations, anions, and natural organic matter are also addressed. The combination of Cu-based catalyst/PMS systems with other advanced oxidation technologies is also discussed. Following that, the degradation mechanisms in the Cu-based catalyst-activated PMS system are considered and synopsized. Lastly, potential future research avenues are proposed to enhance the technology and offer support for developing of economically viable materials based on copper for activating PMS.

Keywords: advanced oxidation process; copper-based catalyst; degradation mechanisms; organic pollutants; peroxymonosulfate activation

check for updates

Citation: Bouzayani, B.; Lomba-Fernández, B.; Fdez-Sanromán, A.; Elaoud, S.C.; Sanromán, M.Á. Advancements in Copper-Based Catalysts for Efficient Generation of Reactive Oxygen Species from Peroxymonosulfate. *Appl. Sci.* **2024**, *14*, 8075. https://doi.org/10.3390/app14178075

Academic Editor: Dae Sung Lee

Received: 14 August 2024
Revised: 27 August 2024
Accepted: 3 September 2024
Published: 9 September 2024

1. Introduction

Environmental contamination has indeed been recognized as a significant challenge confronted by human beings since the 20th century, and it continues to be a pressing issue today. Pollution is defined as the introduction of contaminants or detrimental substances into the environment, which can cause harmful impacts to human health, living organisms, and even ecosystems. In the case of water pollution, these negative effects are further intensified by the growing demand for water from citizens, agriculture, and industries [1,2]. In recent decades, organic substances have been detected, due to the continuous development of analytical techniques, with increasing frequency in concentrations ranging from ng/L to µg/L in groundwater, urban wastewater, surface water, and drinking water [3]. These substances are known by various names, the most used and recognized being "emerging contaminants". This class of compounds is defined as chemicals of synthetic or natural origin or microorganisms that are not commonly monitored in the environment but that may have adverse effects on the environment or human health [4]. This category includes pharmaceutical and personal care products, pesticides, heavy metals, and industrial chemicals [5]. Additionally, pathogens, including bacteria, viruses, protozoa, and parasites, represent a major concern for water pollution, as these microorganisms can cause serious diseases and even death [6]. The spread of antibiotic-resistant bacteria through contaminated water sources further complicates public health efforts, since these can be transmitted

to humans, particularly affecting those with chronic conditions [7]. Additionally, these compounds disrupt ecological balances, affecting the development and reproduction of aquatic species [8].

To confront the problem, diverse technologies have been developed. Among them, advanced oxidation processes (AOPs) have become increasingly important in addressing the challenges of water pollution. Their ability to degrade recalcitrant pollutants such as drugs and personal hygiene products [9], organic micropollutants [10], and pesticides [11] and provide environmental protection make them a valuable tool in modern wastewater treatment strategies. Among the various AOPs, peroxymonosulfate (PMS)-based AOPs have received intensifying attention for environmental remediation by reason of the powerful generation of hydroxyl radical ($HO^{\bullet}$, standard potential = 2.0–2.8 V versus standard hydrogen electrode vs. NHE), sulfate radical ($SO_4^{\bullet -}$ 2.5–3.1 V vs. NHE), or singlet oxygen ($^1O_2$, 2.2 V vs. NHE) [12,13]. In fact, PMS might be activated through different methods such as thermal activation [14], ultraviolet light (UV) activation [15], photocatalysis [16], electrochemical methods [17], ultrasound irradiation [18], and transition metals [19–21]. Among the previously highlighted activation methods, the use of transition metal-derived catalysts for PMS activation has been recognized as a promising advanced oxidation technique with significant potential for organic decontamination. These catalysts are based on, or derived from, transition metals located in the d-block of the periodic table, such as iron (Fe), copper (Cu), cobalt (Co), and nickel (Ni), among others. They are known for their unique catalytic properties, including multiple oxidation states and the ability to form complexes with various ligands. Additionally, they exhibit robust catalytic activity, offer potential for reuse through recycling, and are cost-effective. Moreover, among the transition metals, Cu has been considered particularly effective in activating PMS [22] due to several compelling reasons that give it an advantage over Fe, which is also commonly used in such processes.

One of the key advantages of Cu over Fe is its ability to operate effectively over a wider pH range. While Fe-based systems tend to be more effective in acidic conditions, Cu-based systems maintain high catalytic activity in neutral and even alkaline environments. This versatility makes Cu a more suitable choice for the various environmental conditions encountered in real-world applications. In addition, Cu exhibits lower toxicity and environmental risk compared to other transition metals such as Co. Although Fe is less toxic and more abundant, the efficiency of Cu in activating PMS often exceeds that of Fe, particularly in generating a higher reactive oxygen species (ROS) yield. In addition, the lower cost of Cu and its effectiveness in removing organic compounds and disinfecting pathogens present an economical and safe alternative, especially when considering the potential risks associated with Fe-based systems, such as the formation of iron sludge.

Recent advances have also focused on improving the performance of Cu-based catalysts by developing heterogeneous systems, which further mitigate the problems related to metal leaching and secondary contamination. These innovations have made Cu not only a practical but also an environmentally responsible option for PMS activation. Different forms of heterogeneous Cu-based catalysts have been widely investigated thus far, encompassing zero-valent copper (ZVCu) [23], copper oxides [24,25], and magnetic copper ferrite [26]. Table 1 summarizes the removal performance of emerging contaminants through the catalytic activation of PMS by ZVCu, copper oxide, and copper ferrite. In addition to these heterogeneous Cu-based catalysts, other catalysts with more unique and specific properties have also been developed, and they are referred to as Cu-based designed catalyst materials. Advances in the design of Cu-based catalysts, such as the development of core–shell structures, layered double hydroxides (LDHs), and metal–organic frameworks (MOFs), have shown promise in enhancing the stability of the catalyst and preventing copper leaching. These materials are engineered to maintain their catalytic activity while minimizing dissolution into the water, thereby mitigating secondary pollution. All these mentioned catalysts are explained in more detail in the respective subsections of Section 2.

Table 1. ZVCu, copper oxide, and copper ferrite catalysts for the degradation of organic pollutants by PMS activation.

Catalyst	Contaminant	Reactive Species	Efficiency	Ref.
ZVCu				
Nanoscale ZVCu	Benzoic acid (BA)	$SO_4^{\bullet-}$, $HO^{\bullet}$	100% in 10 min	[27]
ZVCu	2,4-DCP	$SO_4^{\bullet-}$, $HO^{\bullet}$	56.7% of TOC in 120 min.	[28]
ZVCu	NPX	$SO_4^{\bullet-}$, $HO^{\bullet}$	91.0% in 30 min	[29]
Copper oxide				
CuO	Iopamidol	$SO_4^{\bullet-}$, $HO^{\bullet}$	100% in 15 min	[30]
CuO	Phenol	$SO_4^{\bullet-}$, $HO^{\bullet}$	65% in 60 min	[31]
CuO	BPA	$^1O_2$, $SO_4^{\bullet-}$	100% in 20 min	[32]
Cu_2O	BPA	Surface-activated PMS	100% in 120 min	[33]
CuO	AO7	$SO_4^{\bullet-}$, $HO^{\bullet}$	95.38% in 15 min	[34]
Spongelike porous CuO	AO7	$SO_4^{\bullet-}$	85% in 60 min	[35]
Copper ferrite				
$CuFe_2O_4$	TBBPA	$SO_4^{\bullet-}$, $HO^{\bullet}$	99% in 30 min	[36]
$CuFe_2O_4$	ATZ	$SO_4^{\bullet-}$, $HO^{\bullet}$	>98% in 15 min	[37]
$CuFe_2O_4$	BPA	$SO_4^{\bullet-}$, $HO^{\bullet}$	95.2% in 60 min	[38]
$CuFe_2O_4$	Norfloxacin	$SO_4^{\bullet-}$, $HO^{\bullet}$	>90% in 120 min	[39]
$CuFe_2O_4$	Iopromide	$SO_4^{\bullet-}$, $HO^{\bullet}$	~100% in 10 min	[40]
$CuFeO_2$	Sulfadiazine (SDZ)	$SO_4^{\bullet-}$, $HO^{\bullet}$	86% in 12 min	[41]
$CuFeO_2$	Orange I	$SO_4^{\bullet-}$, $HO^{\bullet}$	77.8–79.3% in 30 min	[42]

Therefore, this review intends to provide the most recent overview of multiple Cu-based catalysts for activating PMS. Moreover, methods used to assess the activation of PMS with copper-based catalysts are outlined. Afterwards, diverse variables influencing reactivity are examined. Then, the concise introduction of combining Cu-based catalyst/PMS systems with other sophisticated oxidation approaches is provided. The degradation mechanism of the Cu-based catalyst-activated PMS system is summarized and discussed. Finally, we present conclusions and future outlooks.

2. Cu-Based Catalyst-Activated PMS Processes

In the past ten years, Cu-species catalysts have gained much attention to activate PMS owing to their cost-effectiveness and high catalytic potential, leading to the efficient elimination of organic pollutants and to eco-friendliness. Cu can also be a versatile catalyst that is easily combined with other materials such as iron to enhance their catalytic performance.

The use of Cu-based catalysts provides an attractive and practical solution to remove organic pollutants, offering improved efficiency. Heterogeneous catalysts are frequently employed in conjunction with AOPs, such as PMS activation. This combination enhances the efficiency and effectiveness of contaminant degradation [43–47]. Several strategies have been proposed to mitigate Cu leaching; among them, the use of Cu-based catalysts in heterogeneous forms, including natural or designed, is considered one of the most effective strategies. By anchoring Cu onto solid supports, the risk of metal ion release is significantly minimized. These heterogeneous catalysts are also easier to separate from the treated water, reducing the likelihood of secondary pollution. Other strategies are pH control, operating within a neutral to slightly alkaline pH range that reduces the solubility of Cu species, thus limiting their release into the water.

2.1. Zero-Valent Copper

ZVCu finds applications in a wide range of industries, including agriculture [48], catalysis [49], medical sectors [50], and environmental remediation [51]. ZVCu has been valuable for its contributions to pollution abatement initiatives. It is considered a favorable option for the remediation of wastewaters and manufacturing discharge [52–54]. This is correlated with the potential of ZVCu to produce electrons, ionic species (Cu(I) and

Cu(II)), and hydroxides/oxides near the metal surface throughout oxidation–reduction processes [55,56]. To eliminate pollutants near the metal surface, both reductive and oxidative processes are employed. The layer covering the ZVCu surface, composed of Cu oxides/hydroxides, enhances the degradation process through adsorption. However, there are certain pollutants that cannot be efficiently degraded using only ZVCu. For this reason, adding an oxidizing agent and even using irradiation sources are some of the substitutes implemented to improve the effectiveness of the ZVCu. On the other hand, PMS is a potent oxidizing agent. It is characterized by high stability, relatively low cost, and excellent aqueous solubility. Because of its non-symmetrical arrangement, which makes it more easily activated by an assortment of catalysts, PMS has attracted increasing interest as a substitute for hydrogen peroxide (H_2O_2) and peroxydisulfate ($S_2O_8^{2-}$). Additionally, activating PMS offers multiple advantages such as moderate reaction parameters and the preclusion of subsequent pollution [57], and it is currently regarded as an outstanding option for the degradation of persistent organic compounds. Despite the pros, there are some shortcomings associated with the rate of reactions between PMS and organic pollutants at room temperature, requiring activation to expedite the procedure [58]. For this reason, there are many methods used. Nevertheless, the preferable technique is one that can significantly enhance efficiency, requiring less energy to initiate the activation process and being cost-effective compared to other activation methods. The utilization of metallic transition elements for activating PMS demonstrates significantly enhanced activation rates and user-friendliness. Many studies have indicated the performance of the combination of PMS with ZVCu [28,59,60]. The effectiveness of the coupling is associated with the production of extremely high levels of ROS such as $SO_4^{\bullet-}$ or $HO^{\bullet}$ [61]. ROS are powerful oxidants and can participate in the breakdown of pollutants in various environmental applications. Some research indicates that both radicals can coexist in the system, with elimination effectiveness linked to the generation of both species [62] or a predominant one [63]. Thus, in Figure 1, the ZVCu/PMS system can exhibit synergistic effects. PMS can activate ZVCu by transferring an electron to the ZVCu surface, generating Cu(I) species. These Cu(I) species can act as intermediates in catalytic reactions, facilitating the transformation of organic compounds.

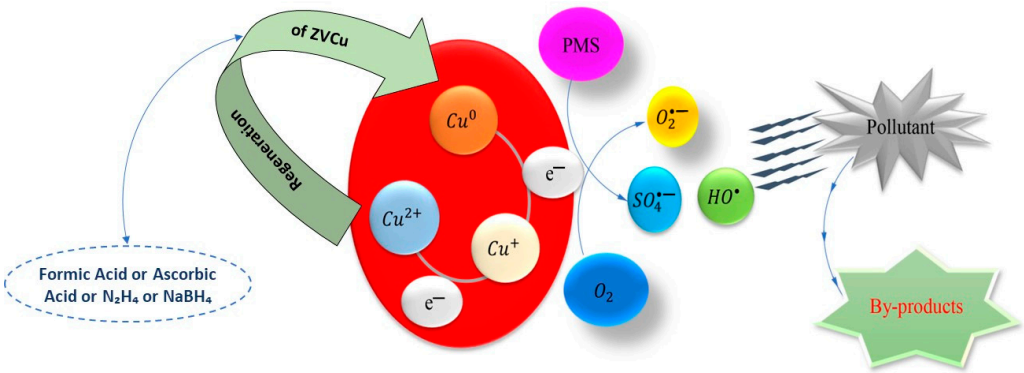

Figure 1. Behavior model of ZVCu/PMS in solution proposed for pollutant degradation.

The reaction pH may influence the concentration of a particular species. Under alkaline conditions, the $SO_4^{\bullet-}$ might undergo a reaction with the hydroxyl anion, leading to the production of the $HO^{\bullet}$ radicals (Equation (1)) [64].

$$SO_4^{\bullet-} + HO^- \leftrightarrow HO^{\bullet} + SO_4^{2-} \quad (1)$$

Zhou et al. [27] assessed the use of ZVCu as a catalyst for activating PMS in the elimination of benzene carboxylic acid (20 μmol L^{-1}). In this investigation, the corrosion of the transition metal was hastened by PMS via Equation (2). The proposed degradation mechanism resembled the one used with hydrogen peroxymonosulfate (HSO_5^-).

$$2Cu^0 + HSO_5^- \leftrightarrow 2Cu^+ + OH^- + SO_4^{2-} \quad (2)$$

To eliminate 2,4-dichlorophenol (2,4-DCP), Zhou et al. [28] utilized the ZVCu/PMS system. Under acidic conditions, the examination of the mechanism demonstrated that PMS accelerates ZVCu corrosion, releasing Cu(I). The produced Cu(I) can induce the production of ROS through chain reactions with oxygen or activate PMS. $SO_4^{\bullet-}$ and $HO^\bullet$ radicals are among the ROS that participate in the elimination of 2,4-DCP. The steps involved in the removal process of the phenol derivative comprise dechlorination, dehydrogenation, hydroxylation, ring opening, and mineralization. Another study by Ghanbari et al. [65] evaluated the effectiveness of ZVCu in the decomposition of H_2O_2 and HSO_5^- for the removal of textile effluents. PMS/ZVCu exhibited higher efficiency in removing chemical oxygen demand and total organic carbon (TOC) compared to the H_2O_2/ZVCu combination. Nevertheless, the authors did not scrutinize the species participating in the elimination to suggest a reaction mechanism model. Chi et al. [29] examined the triggering of PMS using four distinct types of ZVCu, namely, copper foam, copper sheets, graphene–copper sheets, and graphene–copper foam, for the evaluation of the degradation mechanism of naproxen (NPX). ZVCu coated with graphene resulted in a 30% decrease in Cu^{2+} release and a 10% increase in NPX elimination efficiency. Additionally, electron spin resonance (ESR) and radical-scavenging analysis studies verified that hydroxyl radicals were the prevailing species accountable for the breakdown rather than sulfate radicals.

It should be highlighted that the main advantages of ZVCu are its high capacity to generate $SO_4^{\bullet-}$ and $HO^\bullet$ radicals and its relatively low-cost and easy production process, making it an attractive option for environmental remediation. Its versatility allows it to function effectively across a range of environmental conditions, and it can be employed in both reductive and oxidative processes. However, as previously mentioned, a significant limitation is the potential leaching of copper ions into the treated water, which could pose environmental risks. Furthermore, the efficiency of ZVCu may decline over time due to surface passivation, which can reduce its catalytic activity.

2.2. Copper Oxide

Copper oxide refers to a compound composed of copper and oxygen. It has several important properties and applications. Copper oxide, as a reliable, cost-effective, and low-toxicity heterogeneous catalyst, exhibits an excellent catalytic efficiency [66]. CuO is recognized as being among the most significant catalysts and a strong contender to trigger PMS [30,67–69]. Evaluating the two most stable copper oxide catalysts (CuO and Cu_2O), the catalytic activity of CuO is higher than that of Cu_2O [70,71].

Ji et al. [72] synthesized CuO for phenol degradation in aqueous solution via PMS activation. The findings indicated that the prepared CuO was proficient in catalyzing the decomposition of PMS into $SO_4^{\bullet-}$ and $HO^\bullet$, demonstrating its effectiveness for phenol elimination. In this research, it was assumed that $SO_4^{\bullet-}$ and $HO^\bullet$ are produced directly from the reaction, in which Cu^{2+} is initially reduced to Cu^+ by HSO_5^- [73]. The outstanding catalytic performance of copper oxide in activating PMS has been well recognized. However, directly using CuO as a catalyst for activating certain oxidants in an aqueous solution still requires more attention because of the leaching of Cu^{2+} ions; CuO can only work efficiently within a limited pH range [72], and the catalysts are difficult to separate from the reaction system [73]. Zhang et al. [73] compared the stability of copper oxide and copper-substituted ferrite and reported that only 1.5 ± 0.1 μg·L^{-1} of Cu ions leached from CuFeO, whereas 46 ± 3 μg·L^{-1} leached from CuO, using identical parameters after catalytic PMS activation. This demonstrates that CuO exhibits lower stability and efficiency in redox processes as a metal catalyst. Nevertheless, the issues with the dissolution and aggregation of the copper ions curtail the real-world use and reduce the activity of copper oxide. Addressing such shortcomings and further improving the powdered CuO catalyst can be accomplished by integrating the metal oxide onto a substrate with high stability, strong adsorption affinity, and high surface area toward the contaminant, such as zeolite [74,75],

carbon fibers [76], and polymers [77]. To reduce CuO aggregation and increase its specific surface area for catalytic reactions, Du et al. [31] evaluated the catalytic performance of CuO/reduced graphene oxide (rGO) and reported that it exhibited much higher catalytic efficacy compared to CuO during the removal of 2,4,6-trichlorophenol. Kiani et al. [40] found that activated carbon-supported CuO could be recycled for three cycles, and the release of copper ions was insignificant. Li et al. [78] synthesized a composite of CuO supported on biochar as a PMS activator for acid orange 7 (AO7), methylene blue, atrazine (ATZ), rhodamine B (RhB), and ciprofloxacin removal in highly saline organic wastewater, which achieved excellent catalytic efficacy. All these findings indicated that incorporating CuO onto the supporter is an effective method for enhancing its catalytic performance.

In terms of advantages, CuO is a stable catalyst that can be easily integrated into composite materials to enhance its performance. However, one of the main disadvantages of CuO is its tendency to leach copper ions into the water, which can limit its long-term applicability and may require additional treatment steps to mitigate this issue. Additionally, CuO's effectiveness is highly dependent on precise pH control, as its catalytic activity can significantly diminish outside of the optimal pH range.

2.3. Magnetic Copper Ferrite

The heterogeneous spinel-type ferrites MFe_2O_4 (M=Co, Zn, Ru, Cu, Ni, Mn, etc.) have garnered notable interest due to their remarkable properties, including relatively high activation performance, specific structure, outstanding recyclability, and stability, in addition to magnetic retrieval capability [41,79,80]. Among them, copper ferrite ($CuFe_2O_4$) has been extensively researched for its ferromagnetic characteristics and inherent surface hydroxyl sites. It combines the benefits of Cu and Fe, offering a synergistic effect that enhances ROS generation and pollutant degradation. Its magnetic properties allow for easy separation and recovery from the treated water, making it highly reusable and cost-effective. $CuFe_2O_4$ also exhibits high stability and efficiency under a wide range of operational conditions. These materials have been widely studied owing to their effective function in catalyzing PMS for the degradation of persistent pollutants [81,82]. Considering other MFe_2O_4, such as $CoFe_2O_4$, $NiFe_2O_4$, $MnFe_2O_4$, $ZnFe_2O_4$, etc., even though its catalytic efficiency is relatively low compared to that of $CoFe_2O_4$, the low toxicity of $CuFe_2O_4$ makes it a significant activator of PMS [83]. Moreover, a notable linear correlation has been shown between the number of surface hydroxyl sites and the degradation rate [84]. The diversity of preparative methods for obtaining copper ferrite, including the hydrothermal method [85], solid-state reaction method [86], coprecipitation technique [87], sol–gel method [88], sonochemical method [89], microwave (MW)-assisted synthesis method [90], and combustion synthesis method [38], leads to lower operational costs and increased catalytic activity without additional pollution [91]. Therefore, $CuFe_2O_4$ is highly regarded as an excellent catalyst for the elimination of contaminants of organic origin, as indicated by several previous studies. The literature reports several examples of its ability of activate PMS. Figure 2 presents a schematic illustration of the mechanisms of PMS activation by $CuFe_2O_4$.

Xu et al. [36] observed that bisphenol A (BPA) was degraded within 1 h using 0.3 gL^{-1} PMS and 0.6 gL^{-1} $CuFe_2O_4$ at a neutral pH, while the performance of a CuO/PMS system was only 26.1% at the same time. This highlights that $CuFe_2O_4$, as a polymetallic catalyst, exhibits faster and better catalytic performance than single-metal catalysts due to the synergistic effect. A beneficial cycle is created between $Cu^{3+}/Cu^{2+}$and Fe^{3+}/Fe^{2+}, enhancing the generation of radicals and facilitating the smooth removal process. It is notable that surface-bound radicals of $CuFe_2O_4$ were primarily responsible for the removal of BPA with few contributions of radicals in the solution. Ding et al. [37] observed that the $CuFe_2O_4$/PMS system could eliminate 99% of tetrabromobisphenol A (TBBPA) within 30 min. Similarly, Guan et al. [92] reported that 98% of ATZ was removed within 15 min using 1 mM PMS and 0.1 gL^{-1} $CuFe_2O_4$. Additionally, the excellent stability of the chemical composition and surface functional groups of $CuFe_2O_4$, coupled with its reusability, are important advantages that make $CuFe_2O_4$ a competent activator for PMS. It was observed

that even after seven recycling cycles, $CuFe_2O_4$ retained good crystallization and high activity during the degradation of iopromide [73].

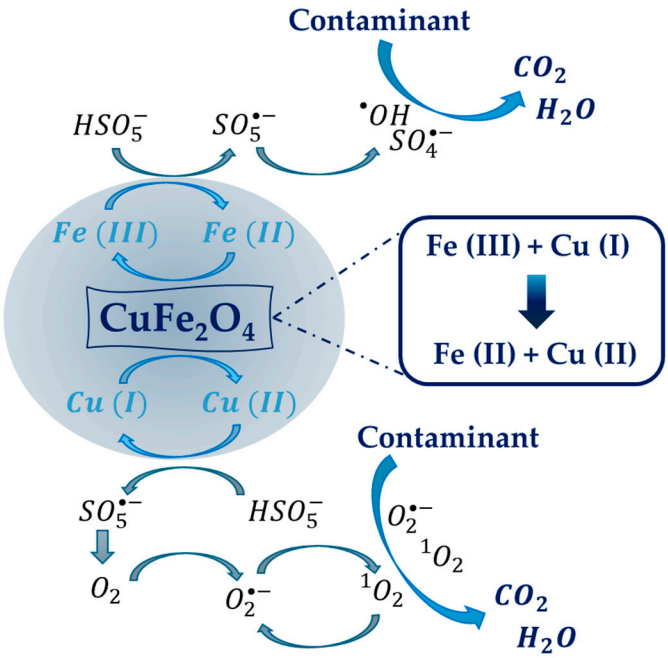

Figure 2. Proposed activation mechanism of the $CuFe_2O_4$/PMS system.

$CuFe_2O_4$ was characterized by Fourier transform infrared spectroscopy before and after reaction. The post-reaction spectrum depicted that the four adsorption bands changed minimally, indicating that the chemical composition and structure of $CuFe_2O_4$ were not destroyed and that $CuFe_2O_4$ exhibited excellent stability throughout the reaction process [93].

Numerous investigations have reported the performances of $CuFe_2O_4$ spinel and supported $CuFe_2O_4$ catalysts synthesized through coprecipitation and sol–gel methods for activating PMS [41,92,94]. $CuFe_2O_4$ is catalytically more stable than $CuFeO_2$, which has additionally been employed to produce $SO_4^{\bullet-}$ from PMS in a recent investigation [95]. The choice of an appropriate synthesis technique is crucial for the efficient preparation of the catalyst. For instance, solvothermally prepared $CuFe_2O_4$, (with organic solvent and surfactant) shows decreased catalytic activity and organic compound release compared to the catalyst fabricated without employing any organic ingredients [96].

In relation to the PMS activation, $CuFe_2O_4$ as a Cu–Fe mixed-metal catalyst imparts synergistic redox reactions to the surface for Cu^{3+}/Cu^{2+}, Cu^{2+}/Cu^{+}, and Fe^{3+}/Fe^{2+} in a tetrahedral and/or octahedral structure to optimally produce $SO_4^{\bullet-}$ radicals from PMS via the following mechanism (Equations (3)–(7)):

$$Cu^{2+} + HSO_5^- \rightarrow Cu^{+} + SO_5^{\bullet-} + H^{+} \quad (3)$$

$$Cu^{+} + HSO_5^- \rightarrow Cu^{2+} + SO_4^{\bullet-} + OH^{-} \quad (4)$$

$$Cu^{+} + Fe^{3+} \rightarrow Cu^{2+} + Fe^{2+} \quad (5)$$

$$Fe^{3+} + HSO_5^- \rightarrow Fe^{2+} + SO_5^{\bullet-} + H^{+} \quad (6)$$

$$Fe^{2+} + HSO_5^- \rightarrow Fe^{3+} + SO_4^{\bullet-} + OH^{-} \quad (7)$$

X-ray photoelectron spectroscopy provides evidence of the transformation in the Cu oxidation state transitioning from Cu^{2+} to a blend of Cu^{2+}/Cu^{+} in $CuFe_2O_4$ pre-reaction and post-reaction [97]. The synergistic effect between cupric cations and ferric cations is clearly apparent. Since the generated Cu^{+} (Equation (3)) could undergo disproportionation readily (e.g., with molecular oxygen), electron transfer from Cu^{+} to Fe^{3+} (Equation (5))

produces Fe^{2+}, which shows greater thermodynamic stability against disproportionation. Therefore, this process enhances the generation of $SO_4^{\bullet-}$ from PMS [98].

$$4Cu^{+} + O_2 + 4H^{+} \rightarrow 4Cu^{2+} + 2H_2O \quad (8)$$

$$4Fe^{2+} + O_2 + 4H^{+} \rightarrow 4Fe^{3+} + 2H_2O \quad (9)$$

It is noteworthy that the one–electron transition of PMS to Cu^{2+} to generate $SO_5^{\bullet-}$ is unfavorable under standard conditions given the standard reduction potentials of Cu^{2+}/Cu^{+} (E° = +0.17 V vs. NHE), $SO_5^{\bullet-}/HSO_5^{-}$ (E° = +1.1 V vs. NHE), and $SO_5^{\bullet-}/SO_5^{2-}$ (E° = +0.81 V vs. NHE) [98]. For the redox reaction to take place, PMS forms a surface complex on the catalyst's surface, potentially by displacing the surface hydroxyl groups. The increased rate of interfacial electron transfer due to the formation of a PMS–metal oxide complex [99] and the relatively low concentration of $SO_5^{\bullet-}$ in the reaction environment lead to lower actual reduction potential values for $SO_5^{\bullet-}/HSO_5^{-}$ and $SO_5^{\bullet-}/SO_5^{2-}$ in real aqueous systems. This thermodynamic condition makes the reaction (Equation (3)) feasible [92]. Observations of PMS complexes on metal oxide surfaces have been detected through IR and Raman spectroscopy [41]. Additionally, it is plausible that PMS is activated by $CuFe_2O_4$ via the $Cu^{2+} - Cu^{3+} - Cu^{2+}$($Cu^{3+}/Cu^{2+}$, E° = 2.40 V vs. NHE) redox transition [71].

Cu^{3+}/Cu^{2+} possesses a comparatively elevated standard reduction potential (E° of Cu^{3+}/Cu^{2+} in solution and solid phases are +1.57 vs. NHE and +2.30 V vs. NHE, respectively) [100]. The discrepancies in E° values between the dissolved and solid Cu^{2+} phases provide additional insight into the inferior performance of dissolved Cu^{2+} ions in contrast to heterogeneous Cu^{2+} catalysts.

One of the main disadvantages of $CuFe_2O_4$ is that its catalytic activity can be lower compared to that of other metal ferrites such as $CuFe_2O_4$. Additionally, the synthesis of $CuFe_2O_4$ is often more complex and costly, which can limit its widespread adoption. Despite these challenges, $CuFe_2O_4$ is particularly valuable in the treatment of complex wastewater streams, where its magnetic properties enable easy recovery and reuse. It is also effectively employed in hybrid AOPs that require enhanced pollutant degradation.

2.4. Cu-Based Designed Catalyst Materials

In recent years, the use of Cu-based catalysts for PMS activation has significantly increased, as discussed in previous sections. However, researchers have also explored other alternatives to further enhance the properties of these catalysts. This exploration has led to the development of advanced materials with improved characteristics such as increased specific surface area, high stability, and tunable internal structure. Notable among these materials for PMS activation are MOFs, LDHs, and deep eutectic solvents (DESs) [101–103].

2.4.1. Cu-Based MOFs

Regarding MOFs, these materials are composed of metal ions coordinated with organic ligands, forming a highly porous three-dimensional structure. These materials are notable for their high stability and tunable internal structure [104,105].

Due to the wide variety of MOFs, they can be classified according to their structure and composition. This review focuses on copper-containing MOFs, commonly referred to as Cu-MOFs. They are usually composed of copper ions or groups coordinated with organic linkers, creating a robust and tunable framework. The synthesis of Cu-MOFs can be achieved through several methods, each of which offers different advantages and is suitable for different applications. The choice of the synthesis method depends on the desired properties of the MOF, the specific application, and the scalability requirements. The most employed techniques for synthesizing Cu-MOFs are:

- Solvothermal synthesis: This is the most widely used method to produce Cu-MOFs. In this technique, the copper salts and organic linkers are dissolved in a solvent and heated in a sealed container (often an autoclave) at elevated temperatures, typically in the range of 80° C to 220° C. The solvothermal conditions facilitate the self-assembly

of the metal ions and organic linkers into the desired structural structure [106]. This method allows for precise control over the size, morphology, and crystallinity of the MOFs by adjusting parameters such as temperature, reaction time, and solvent type.

- MW-assisted synthesis: This offers a fast and energy-efficient approach to producing Cu-MOFs. This method involves the use of MW radiation to heat the reaction mixture, significantly reducing the synthesis time compared to conventional solvothermal methods. MW-assisted synthesis can improve the nucleation and growth rates of MOFs, leading to high-quality crystalline materials with uniform particle sizes [107]. The rapid heating and cooling cycles provided by MW irradiation also help to minimize the formation of defects within the MOF structure.
- Electrochemical synthesis: This is an emerging technique for producing Cu-MOFs, where an electric current is applied to drive the assembly of the framework. In this method, a copper anode is dissolved to release copper ions in an electrolyte solution containing organic linkers. The electric field promotes the interaction between the copper ions and the linkers, which results in the formation of the MOF on the electrode surface [108]. Electrochemical synthesis is advantageous for producing thin films of MOF directly on conductive substrates, which makes it suitable for applications in sensors and electronic devices.
- Sonochemical synthesis: This uses ultrasonic waves to induce chemical reactions and facilitate the formation of copper MOFs. The ultrasonic waves generate high temperatures and localized pressures within the reaction mixture, improving the reaction kinetics and promoting the formation of the MOF structure [109]. This method is known for its simplicity, fast reaction times, and ability to produce MOFs with unique morphologies and improved surface areas.
- Mechanochemical synthesis: This involves the use of mechanical force to induce chemical reactions between copper salts and organic linkers. This technique typically employs grinding or ball milling to physically mix and activate the reactants, leading to the formation of the MOF structure without the need for solvents or high temperatures [110]. Mechanochemical synthesis is environmentally friendly and scalable, which makes it a promising approach for the large-scale production of Cu-MOFs.

However, it is also possible to combine several of these synthesis processes to improve the properties of Cu-MOFs. Additionally, another advantage of combining these processes is that the synthesis times and solvent volumes can be reduced, resulting in a material with better properties compared to using a single process. For example, the combination of the MW-assisted and solvothermal methods can result in a hierarchical porous structure that provides a larger specific surface area, better thermal and chemical stability, and increased adsorption capacity [111].

In relation to the applicability of Cu-MOFs as catalysts for PMS, the literature reports several examples such as those summarized in Table 2. For example, an ultra-thin Cu-TCPP(BA)-MOF synthesized by Bai et al. [112] exhibits high efficiency in PMS activation under visible light, completely degrading 10 ppm of RhB in 40 min through the non-radical species $^1O_2$ [112]. The generation of $^1O_2$ and $HO^\bullet$ radicals is attributed to the Cu-TCPP(BA)-MOF transitioning from Cu(I) to Cu(II) when irradiated with visible light, producing h^+. This process, in reaction with the HSO_5^-, triggers multiple reactions that result in the formation of superoxide, hydrogen peroxide, and $SO_5^{\bullet-}$, leading to a significant production of $^1O_2$. Additionally, this system can eliminate various organic pollutants such as tetracycline and phenol under conditions of 0.1 $g{\cdot}L^{-1}$ of PMS and 0.1 $g{\cdot}L^{-1}$ of catalyst at neutral pH. It also effectively inactivates pathogens such as *Escherichia coli* (*E. coli*), achieving the complete inactivation of 10^7 colony-forming units per mL ($CFU{\cdot}mL^{-1}$) in just 50 min.

Moreover, some Cu-MOFs for the activation of the PMS can follow other pathways such as the generation of $SO_4^{\bullet-}$ and $HO^\bullet$ radicals. One example is the Cu-MOF modified with Fe^{+3} ions synthesized by Quan et al. [113], which improved degradation efficiency due to the increased ion exchange within the MOF and the reduction of coordinated

water molecules thanks to the presence of this ion. Modification with different long-chain quaternary ammonium bromides established a hydrophobic microenvironment, favoring the removal of non-steroidal anti-inflammatory drugs such as diclofenac, NPX, and ibuprofen. The best PMS activation was achieved with the MOF modified with hexadecyltrimethylammonium bromide, achieving a 90% removal of diclofenac in 120 min. However, the removal of other non-steroidal anti-inflammatory drugs, such as ibuprofen and NPX, did not exceed 30%. Although it was not efficient for other drugs of the same class, it showed high stability, with only a 20% reduction in activation after five cycles, demonstrating high durability and reusability, and it was effective in complex waters such as tap water and secondary effluent water. In pursuit of enhancing the stability and usability of Cu-MOFs, Cu-MOF-74 stands out, as synthesized by Zheng et al. [114] through a green synthesis method on a PVDF membrane, resulting in a catalytic membrane reactor. This reactor demonstrated the ability to activate PMS and achieve the complete removal of RhB in 60 min while also efficiently removing other compounds such as methylene blue (89.5%), tetracycline (67.9%), and rifampicin (80.9%).

Additionally, in recent years, new structures have been sought to generate new MOFs. Wu et al. synthesized the MOF $[Cu_3(\mu_3\text{-O})(pypz)_3]NO_3$, which they named MAF-wyu2 because it belongs to the metal-azolate frameworks (MAFs) [115]. The main characteristic of this new MOF is that it possesses rich open metal sites based on the planar trinuclear $[Cu_3(\mu_3\text{-O})]^{4+}$ clusters. This structure allows for higher catalytic activity to activate PMS, as well as remarkable thermal and chemical stability. Unlike other MOFs mentioned previously, the optimal conditions for this process are achieved when the initial pH is above 9, which allows for the complete removal of sulfamethoxazole in 60 min. Additionally, the stability of this MOF is very high, as its catalytic activity remains practically unchanged after five cycles. Figure 3 shows the general scheme of this structure along with the mechanisms involved in the degradation process of an antibiotic like sulfamethoxazole.

However, in recent years, alternatives have been explored to further enhance the catalytic properties and stability of MOFs by incorporating a second metal, resulting in bimetallic MOFs. An example of this type is presented by Li et al. [116] with the synthesis of Cu_1Co_1-MOF-74, which is capable of completely removing methylene blue in 30 min, outperforming other previously described MOFs that did not reach 90% removal. Additionally, studies such as that by Wang et al. [117] demonstrate that MOFs like Fe-Cu-MOF can also eliminate hard-to-degrade organic compounds, such as phenol, in less than 60 min, with a catalytic activity loss of less than 20% after four uses. In both studies, the mechanism for contaminant degradation is due to the generation of $SO_4^{\bullet -}$ and $HO^{\bullet}$ species. In addition to being efficient in the removal of dyes and persistent compounds, as previously mentioned, they are also effective in the disinfection of pathogens such as *E. coli*. In a study conducted by Fdez-Sanromán et al. [118], three different FeCu-MOFs functionalized with amino groups were synthesized, each exhibiting different morphologies and properties due to variations in the synthesis procedure. As depicted in Figure 4, the synthesized MOFs displayed diverse shapes, including rod, spindle, and diamond morphologies, with varying Fe/Cu ratios of 1:1, 2:1, and 3:1, respectively. The study found that FeCu-MOFs with ratios of 2:1 and 3.1, synthesized with the same procedure but using different metal salts, were more suitable for degrading organic compounds such as RhB and a mixture of media formed by sulfamethoxazole and antipyrine when using the MOF/PMS system. The degradation efficiency was further enhanced with the application of UV radiation. Conversely, the FeCu-MOF with a ratio 1:1 exhibited superior disinfection capabilities under the CuFe-MOF/PMS system.

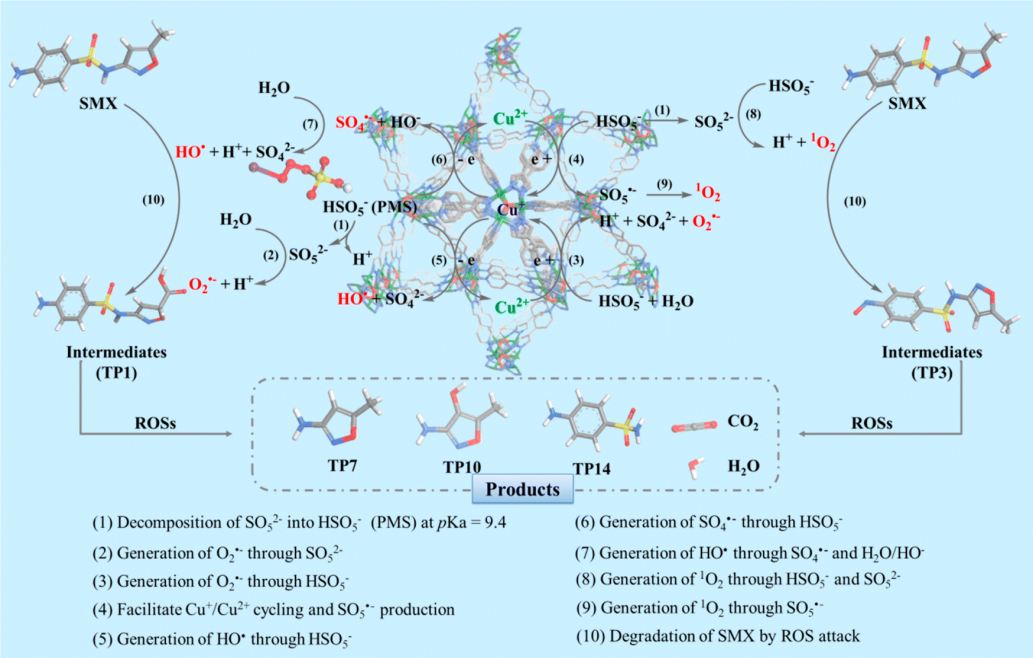

Figure 3. Degradation mechanisms exhibited by MAF-wyu2 for a persistent contaminant like sulfamethoxazole. This figure, reproduced from the study by Wu et al. [115], is used with permission from Elsevier (Amsterdam, The Netherlands), copyright 2024.

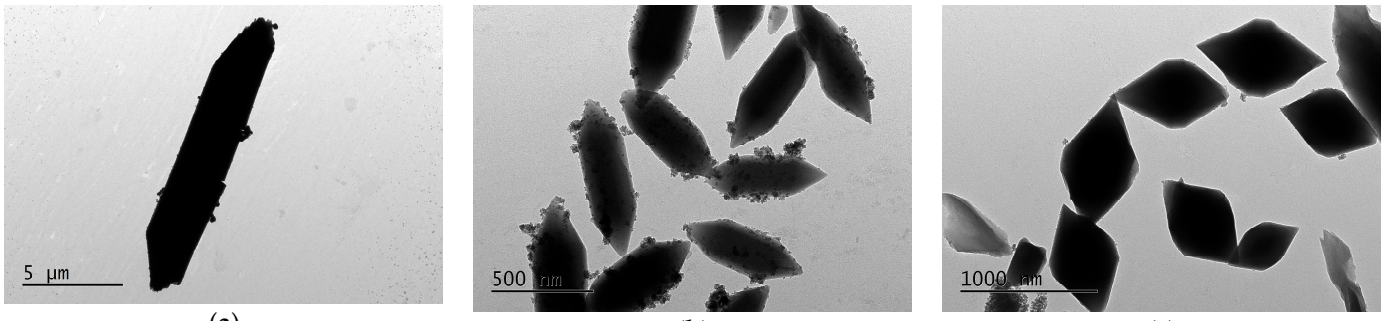

(**a**) (**b**) (**c**)

Figure 4. Transmission electron microscopy images of the different synthesized CuFe(BDC-NH_2) using different procedures and metal salts. Varying the Fe/Cu ratio to 1:1, 2:1, and 3:1, they display diverse shapes, including rod (**a**), spindle (**b**), and diamond (**c**), respectively.

Another alternative is to subject MOFs to various treatments, such as chemical or thermal processes, to obtain MOF derivatives. These derivatives retain many of the properties of the original MOFs while enhancing certain specific properties. A clear example of these MOF derivatives that improve catalytic properties is the nitrogen-doped Cu/carbon material derived from HUKST-1, synthesized by Zhu et al. [119]. In this study, like in the work of Bai et al. [112], the main pathway for the removal of the selected organic contaminant, the antibiotic tetracycline, is through the generation of $^1O_2$, which contributes up to 70.8% to the elimination of this compound. The modifications made to the material allowed for the complete removal of tetracycline in 60 min, with a degradation rate of 0.096 min^{-1}, compared to 0.0367 min^{-1}, which is the rate achieved by the second-best material synthesized for PMS activation in this study. Additionally, not only can these treatments be applied to monometallic MOFs as previously described, but they can also be applied to bimetallic MOFs. For example, in the work by Ji et al. [120], a bimetallic Cu–Fe MOF embedded in carbon was synthesized. Like in the study conducted by Fdez-Sanromán et al. [118], the authors evaluated the optimal synthesis procedure to achieve controlled

size and growth of the MOF, as well as the subsequent thermal treatment, to obtain the necessary properties to degrade the Reactive Brilliant Red X-3B dye. In this study, the synthesis of the Cu–Fe MOF was carried out in two steps, evaluating the reaction time of each step, with a total duration of 12 h. After optimizing the time required for the MOF synthesis and applying the optimal calcination temperature of 600 °C, they obtained the desired properties to degrade the Reactive Brilliant Red X-3B dye, achieving up to 98% removal for a dye concentration of 50 mg·L^{-1} and 90% for a concentration of 150 mg·L^{-1}. Additionally, this material also showed some stability in its PMS activation capacity, as a reduction in its activation of approximately 16% was observed after five cycles.

More examples of these Cu-MOFs, both monometallic and bimetallic, which demonstrate a high capacity for PMS activation and the removal of persistent organic pollutants and pathogens, are presented in Table 2.

2.4.2. Cu-Based LDHs

Regarding LDHs, these materials are two-dimensional compounds consisting of positively charged metal layers and charge-compensating anions located in the interlayer [121]. They can be represented by the general formula $\left[M^{+2}_{(1-x)}M^{+3}_{x}(OH)_2\right]^{x+}(A^{n-})_{x/n}\bullet m\cdot H_2O$, where M^{+2} is a divalent cation, M^{+3} is a trivalent cation, A^{n-} is the intercalated anion with valence n, and x (the molar ratio of M^{+3} to (M^{+2} + M^{+3})) typically ranges from 0.2 to 0.4 for structural stability [122]. In Cu-based LDHs, the presence of low-valent Cu^{+} species within the LDH structure can facilitate electron transfer on the catalyst surface, accelerating the activation of active species.

For the synthesis of Cu-LDHs, several methods discussed in previous sections are employed, with particular emphasis on the solvothermal and MW methods. However, the most widely used synthesis process is coprecipitation, which is the method employed in all the studies described below and in Table 2. Coprecipitation synthesis involves mixing metal salts, controlling the temperature of the mixture, and adding a precipitating agent, typically a base like NaOH, to adjust the pH conditions. This method facilities the easy incorporation of different cations and anions, which is essential for tailoring the properties of LDHs to specific applications.

Table 2. Cu-based designed catalysts for the degradation of organic pollutants and disinfection by PMS activation.

Catalyst	Contaminant	Reactive Species	Efficiency and Reusability	Ref.
HKUST-1	*Saccharomyces cerevisiae* (>10^5 CFU·mL^{-1}) *Geotrichum candidum* (>10^5 CFU·mL^{-1})	-	100% in 25 h >79% in 25 h	[123]
HKUST-1	*E. coli* (10^{10} CFU·mL^{-1})	$SO_4^{\bullet-}$, $HO^{\bullet}$	100% in 30 min 4 cycles, 100%	[124]
FeCu-MOF	Methylene blue (0.2 mM)	$SO_4^{\bullet-}$	100% in 30 min 3 cycles, 87.1%	[125]
CuCo-MOF	Nimesulide (20 mg·L^{-1})	$SO_4^{\bullet-}$, $HO^{\bullet}$	100% in 25 min	[126]
CuCo-MOF-74	Methylene blue (0.2 mM)	$SO_4^{\bullet-}$	100% in 30 min 5 cycles, 76.4%	[116]
Co1Cu1-MOF	Tetracycline (20 mg·L^{-1})	$SO_4^{\bullet-}$, $HO^{\bullet}$ $^1O_2$, $O_2^{\bullet-}$	98.17% in 30 min 4 cycles, 71.26%	[101]
NH_2–$Fe_{2.4}Cu_1$-MOF in polyacrylonitrile spheres	RhB (10 mg·L^{-1})	$SO_4^{\bullet-}$, $HO^{\bullet}$	80.92% in 90 min 5 cycles, >77%	[127]

Table 2. *Cont.*

Catalyst	Contaminant	Reactive Species	Efficiency and Reusability	Ref.
Co_2Cu_1-LDH	Lomefloxacin (10 mg·L^{-1})	$SO_4^{\bullet-}$, $HO^{\bullet}$	96.2% in 30 min 10 cycles, >95%	[102]
MgCuFe-LDH	RhB (5 mg·L^{-1}) Acetaminophen (5 mg·L^{-1})	$SO_4^{\bullet-}$, $HO^{\bullet}$	97.6% in 25 min 93% in 20 min	[128]
Cu-Co-Fe-LDH	Nitrobenzene (2 mg·L^{-1})	$SO_4^{\bullet-}$ at pH < 7 $HO^{\bullet}$ at pH > 9	100% in 6 min 5 cycles, >87%	[129]
CuMn-LDH	BPA (5 mg·L^{-1})	$^1O_2$, $O_2^{\bullet-}$	100% 90 min 4 cycles, >95%	[130]
CoCu-LDH	Sulfamethoxazole (10 mg·L^{-1})	$SO_4^{\bullet-}$, $HO^{\bullet}$	86.6% in 60 min	[131]
CoCu-LDH@polyvinylidene fluoride (PVDF)	Sulfamethoxazole Sulfacetamide Lomefloxacin Carbamazepine (each 10 mg·L^{-1})	$SO_4^{\bullet-}$, $HO^{\bullet}$	92.8% in 60 min 89.6% in 60 min 97.1% in 60 min 91.8% in 60 min	[131]
CuCoFe-LDH coated on biochar	Phenanthrene (1 mg·L^{-1})	$SO_4^{\bullet-}$, $HO^{\bullet}$	96.5% in 15 min 4 cycles, >80%	[132]
CuCoFe-LDH	Glyphosate (100 mg·L^{-1})	$SO_4^{\bullet-}$	99.54% in 5 min 5 cycles, 90.34%	[133]
CuO nanoparticles–DES (DL-menthol/Fenchyl alcohol)	RhB (20 mg·L^{-1})	$SO_4^{\bullet-}$, $HO^{\bullet}$	98% in 18 min	[134]
Cu-BDC * MOF-DES (Choline chloride/urea)	AO7 (30 mg·L^{-1})	-	99% in 120 min	[135]

* BDC: benzene dicarboxylic acid.

The coprecipitation process is typically carried out under controlled pH conditions to ensure the formation of lamellar metal hydroxides. The concentration of metal salts, the rate of addition of the precipitating agent, and the reaction temperature are critical parameters that influence the final structure and properties of the Cu-LDH. The main advantage of coprecipitation is its simplicity and the ability to produce large quantities of material with uniformity.

Unlike the MOFs described in Section 2.4.1, LDHs are usually bimetallic and even trimetallic, meaning they can incorporate two or three different types of metal cations into their structure. This feature allows for greater versatility in modulating their physical and chemical properties, such as ionic exchange capacity, thermal stability, and catalytic activity. Additionally, LDHs have a layered structure that facilitates ionic exchange and the intercalation of organic and inorganic molecules, further expanding their range of potential applications.

For instance, in the study of Xie et al. [130], a Cu_3Mn-LDH is synthesized via coprecipitation, a commonly used method for LDH synthesis. During this process, hydrogen peroxide is incorporated to slightly modify the structure and enhance PMS activation efficiency. Specifically, using 0.1 g·L^{-1} of Cu_3Mn-LDH and 0.25 g·L^{-1} of PMS results in the complete degradation of a 10 mg·L^{-1} concentration of BPA in less than 60 min at neutral pH. This material exhibits a bipath degradation mechanism, with the primary pathway being the generation of $^1O_2$ and the auxiliary pathway involving free radicals, as determined by electron paramagnetic resonance (EPR) analysis and quenching experiments. The generation of $^1O_2$ is the predominant pathway in the degradation of BPA.

Regarding trimetallic LDHs, Zhu et al.'s study highlighted the differences between the metal salts involved in the formation of the LDH structure by synthesizing MgCuFe-LDH, MgCuAl-LDH, and a bimetallic MgFe-LDH [128]. From the synthesis of these three LDHs, it was concluded that the two trimetallic LDHs exhibited a higher degradation capacity compared to the bimetallic one. Among the two trimetallic LDHs, MgCuFe-LDH demonstrated the highest degradation rate, with a 2.9% higher rate than MgCuAl-LDH. This is believed to be due to a significant synergistic effect on PMS activation by the Cu and Fe metals, while Mg provided charge balance and structural stability, enhancing the activation reactions of PMS by Cu and Fe.

Additionally, like MOFs, another approach to further enhance the stability of these catalysts and enable their use in repeated or continuous processes is the formation of membranes or the incorporation of the catalyst onto physical supports. For instance, Guo et al. demonstrated the effectiveness of CoCu-LDH in removing a contaminant like sulfamethoxazole, achieving more than 86% removal in 1 h [131]. However, when this material was immobilized on a support such as PVDF, resulting in CoCu-LDH@PVDF, there was a significant improvement in catalyst activation. In the same timeframe, a removal rate of 92.8% for sulfamethoxazole was achieved. Furthermore, CoCu-LDH@PVDF showed a removal capacity of over 89% for other drugs such as sulfacetamide, lomefloxacin, and carbamazepine. Another approach is to synthesize these LDHs on the structure of other materials, as in the case of Wu et al., who synthesized a trimetallic CuCo-FeLDH on a biochar structure [132]. As shown in Table 2, the results are very promising, with the material displaying high stability over multiple reuse cycles. The successful degradation of phenanthrene is largely attributed to the synergy between the two materials. The biochar, in addition to acting as a support for the LDH, enhances the activation capacity of PMS, allowing its catalytic activity to operate over a broader pH range than without the biochar. Furthermore, this carbon-based material also contributes to PMS activation due to the functional groups it contains. Additionally, a further advantage of combining CuCoFe-LDH with biochar is that it significantly reduces metal leaching, which enhances the material's stability and addresses one of the common issues associated with LDHs.

However, regarding the study of Wu et al. [132], it is important to note that LDHs have some limitations, such as reduced stability upon reuse and insufficient catalytic activity. To address these issues, recent research has focused on developing nanohybrid materials by rGO with LDH. This new material features a periodic morphology combining positive LDH components with intercalated anionic species like rGO. It improves PMS activation, as well as other properties such as conductivity and chemical stability [136]. The first study to synthesize such a copper-based hybrid material was conducted by Shahzad et al. [137]. Their work evaluated this material with various agents, including persulfate and hydrogen peroxide, finding that PMS was the most effective. It achieved the complete removal of BPA within 40 min. Like Xie et al.'s study [130], two degradation pathways were observed: the primary pathway involved singlet oxygen generation through $\bullet O_2$, while the secondary pathway involved $^1O_2$.

More catalysts, both bivalent/trivalent unmodified and modified, as in the previous study, are included in Table 2.

2.4.3. Cu-Based DESs

Recently, increasing environmental concerns have highlighted the need to develop sustainable and clean technologies. Researchers worldwide are actively working to create greener methods for synthesizing catalysts. Their efforts focus on minimizing the use of hazardous solvents during synthesis and purification, avoiding toxic substances, reducing energy consumption, and promoting synthesis under ambient conditions. In this context, DESs that act not only as solvents but also as structure-directing agents stand out [135]. DESs are liquid systems formed by the interaction of two or more components, usually a hydrogen bond donor (HBD) and a hydrogen bond acceptor (HBA), in a molar proportion where a eutectic mixture is formed, resulting in a liquid state with unusual solvent proper-

ties (a melting point lower than that of any of the individual components) [138]. There are different types of DESs depending on the combination of HBA and HBD used. DESs can be described by the general formula of $Cat^+ X^- zY$, where Cat^+ refers to an ammonium, phosphonium, or sulfonium cation; X^- generally represents a halide anion, and Y is Lewis or Brønsted acid (z refers to the number of molecules Y interacting with the anion) [139].

DESs, first introduced by Abbott et al. [140], represent a new class of low-cost and environmentally friendly solvents with great potential to replace traditional catalysts and solvents. They have gained significant attention in recent years due to their remarkable properties, such as high solubility and conductivity, low toxicity, and easy recovery [139,141]. One of the advantages of DESs is their high mutual compatibility with numerous metal salts. Thus, DESs can maximize the incorporation of metal salts used in synthesis into the final product, such as metal oxides [103]. For this reason, and because they are pure green solvents that are environmentally friendly, in recent years, they have proven to be very useful in the synthesis of catalytic materials.

Specifically, there are still not many studies related to synthesized copper catalysts assisted by DESs and PMS. Table 2 highlights some of the copper catalysts synthesized with DESs. Among these, Zhang et al. [134] conducted a remarkable study in which CuO nanoparticles were synthesized using a hydrophobic DES, prepared by mixing DL-menthol with phenyl alcohol in a molar ratio of 1:1 at 70 °C. The ability of the resulting CuO nanoparticles to degrade Rh B was tested, and the experimental results showed that the CuO/PMS system (0.16 $g \cdot L^{-1}$ CuO and 0.13 $g \cdot L^{-1}$ PMS) successfully degraded 98.0% of a 20 $mg \cdot L^{-1}$ Rh B solution at pH 7.0 in 18 min. These findings indicate that the synthesized CuO nanoparticles exhibit excellent catalytic performance for the photodegradation of dye in the presence of PMS, outperforming other reported metal oxide-based catalysts. Recently, Cu–Ag nanostructures were synthesized using a one-step electrodeposition method, where the composition and morphology of Cu–Ag were adjusted by a DES composed of choline chloride and urea [142]. The characterization of this nanocatalyst in a single step confirmed that the electrodeposition of metals from a DES offers a cost-effective and environmentally friendly approach to prepare controllable bimetallic and multimetallic copper catalysts.

However, there are some challenges associated with the use of DESs as catalysts. Their high viscosity can impact reaction kinetics by limiting mass transfer and the diffusion of reagents and products. Additionally, the stability and catalytic activity of DESs may be compromised due to their high sensitivity to water and other impurities [139]. To overcome these problems, research on the DES-assisted synthesis of copper-based catalysts is expanding and gaining significant attention. This interest is driven by the ease of synthesizing these materials from inexpensive and renewable starting materials, their low toxicity, and their biodegradable nature.

In summary, Cu-based designed catalyst materials, including Cu-MOFs, Cu-LDHs, and DES-assisted catalysts, offer several distinct advantages. These catalysts feature highly tunable properties such as increased surface area, improved stability, and enhanced catalytic efficiency. Their ability to be specifically designed to target contaminants makes them highly effective for customized applications, positioning them as a versatile and powerful tool in environmental remediation. However, these advanced materials also come with certain disadvantages. The complexity involved in their synthesis often leads to higher costs and potential scalability issues, which may limit their widespread adoption. Additionally, despite their advanced design, some of these materials may still face challenges related to metal leaching or decreased stability over multiple cycles of use, necessitating further refinement and innovation.

In terms of applications, Cu-based designed catalysts are at the forefront of innovative water treatment technologies. They are particularly valuable in high-value applications such as the degradation of emerging contaminants, the disinfection of pathogens, and in advanced treatment processes that require tailored catalytic properties. Their versatility and effectiveness make them a key component in the development of next-generation environmental technologies.

3. Investigative Methodologies for Assessing PMS Activation with Copper-Based Catalysts

Currently, there are various methodologies to study the ROS generated during the activation of PMS using different transition metal-based catalysts. Although numerous lesser-known methods are being developed and explored, such as detection through spectrofluorimetry or colorimetry techniques [143–145], this review focuses on the most commonly used methods in the investigation of PMS activation.

3.1. EPR and ESR Methods

To investigate PMS activation, the frequently used methods are EPR and ESR. The reason they are used is that they allow for the study of ROS due to their unpaired electrons. However, the immediate identification of active species with ESR or EPR is challenging because of their short life span. Hence, spin-trapping agents are introduced to interact with active species, forming stable spin complexes that can be readily quantified as paramagnetic species using EPR or ESR [146]. For $SO_4^{\bullet-}$, $HO^{\bullet}$, and $O_2^{\bullet-}$, 5,5-dimethyl-1-pyrroline-1-oxide (DMPO) is commonly chosen as the alternative capture agent, thus forming DMPO-$SO_4^{\bullet-}$, DMPO-$HO^{\bullet}$, and DMPO-$O_2^{\bullet-}$ spin complexes [85,146]; $^1O_2$ can be trapped by 2,2,6,6-tetramethyl-4-piperidine (TEMP) to create the spin adduct TEMP-$^1O_2$ [147]. After the adducts are formed, hyphenate splitting constants (HPCs) are calculated employing specialized software associated with EPR technology, and these constants are subsequently assessed against the literature or databases to detect active species [146].

An example of a characteristic EPR spectrum is shown in Figure 5. As explained by Yang et al., Figure 5a illustrates that the TEMP-$^1O_2$ spin adduct shows intense and distinct signals after the addition of the catalyst compared to when only PMS is present [148]. In addition, other points to note from the EPR spectra shown in Figure 5 include that, in the case of DMPO-$HO^{\bullet}$ adduct, a quaternion characteristic peak of 1:2:2:1 (HPC:αN = 14.9 G, αβ-H = 14.9 G) typically appears (Figure 5b); for DMPO-$SO_4^{\bullet-}$ admixtures, the characteristic peaks normally indicate a six-component characteristic peak of 1:1:1:1:1:1 (HPC:αN = 13.51 G, αβ-H = 9.93 G, αγ-H1 = 1.34 G, αγ-H2 = 0.88 G) (Figure 4b) [146,149]. In the case of detecting the DMPO-$O_2^{\bullet-}$ adduct, the EPR spectrum is typically characterized by a six-component peak with a ratio of 1:1:1:1:1:1 (HPC:αN = 14.3 G, αβ-H = 11.2 G, αγ-H1 = 1.3 G) [146]. For the TEMP $^1O_2$ adduct, a ternary characteristic peak of 1:1:1 (HPC:αN = 16.3 G) typically appears (Figure 5a) [146,150].

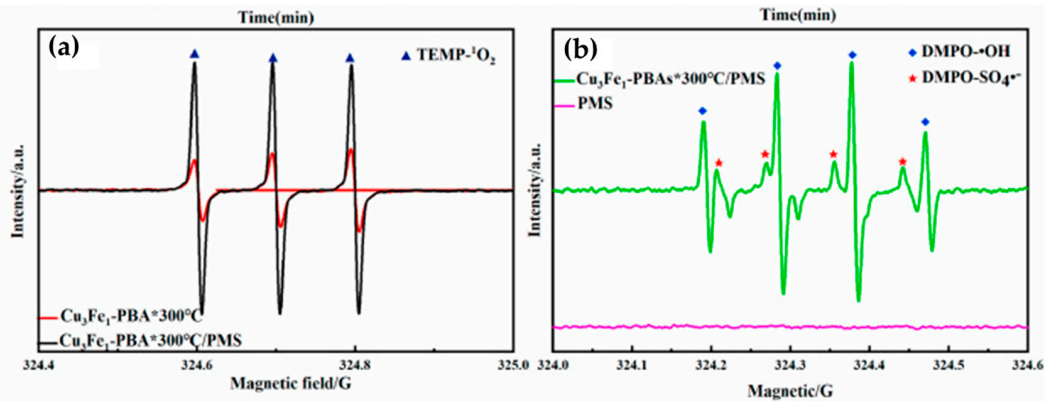

Figure 5. Characteristic EPR spectra are shown based on (**a**) TEMPO for detecting O_2 and (**b**) DMPO as a scavenger for $HO^{\bullet}$ and $SO_4^{\bullet-}$ radicals generated during the PMS activation process, using a Cu–Fe Prussian blue precursor (CuFe-PBA*) as a catalyst. Adapted from [148] copyright 2023 with permission from Elsevier (Amsterdam, The Netherlands).

Furthermore, by analyzing the EPR and ESR peak intensity at different reaction times, the evaluation of various radical species can be performed. For instance, at the beginning of the reaction involving the activation of PMS by $ZnFe_2O_4$ or by MnO_2 for the elimination

of phenol, only $HO^{\bullet}$ is formed (1 min). Subsequently, both $SO_4^{\bullet-}$ and $HO^{\bullet}$ are generated, and the intensity of DMPO-$SO_4^{\bullet-}$ increases progressively as the reaction continues for up to 30 min [151]. Subsequently, only the DMPO-$HO^{\bullet}$ signals persist, as observed at the beginning of the reaction; this indicates that $HO^{\bullet}$ plays a significant role at both the beginning and the end of the reaction.

In some of the preceding publications, the importance of $^1O_2$ was not acknowledged. It remains uncertain whether this oversight resulted from the absence of $^1O_2$ formation in those systems or simply because the authors did not contemplate its potential generation. Newer studies have examined the involvement of $^1O_2$ and demonstrated its significance for certain Cu-based materials [32]. Hence, it could be beneficial to reevaluate certain previously published systems to gain a deeper knowledge of ROS participation.

Nevertheless, the presence of TEMPO signals themselves fails to inherently imply the formation of $^1O_2$. It has been proposed that the TEMP radical cations ($TEMP^{\bullet+}$) produced by an excited photosensitizer could undergo deprotonation and afterward react with molecular oxygen for create TEMPO signals [152,153]. Consequently, even if TEMPO signals are detected, further experiments, like isotope effect experiments, are justified to ascertain if $^1O_2$ is present in the system.

3.2. Radical Quenching

When examining the activation of PMS, radical quenching is a crucial methodology used to understand the behavior and reactivity of radical species formed during the reaction. Basically, quenching agents are added at the beginning of the process to intercept and neutralize the generated radicals. If these radicals are present in the system, they will react with the quenching agents and will not participate in the degradation process. In this way, the involvement of the radicals in the degradation can be determined, as clearly shown in Figure 6.

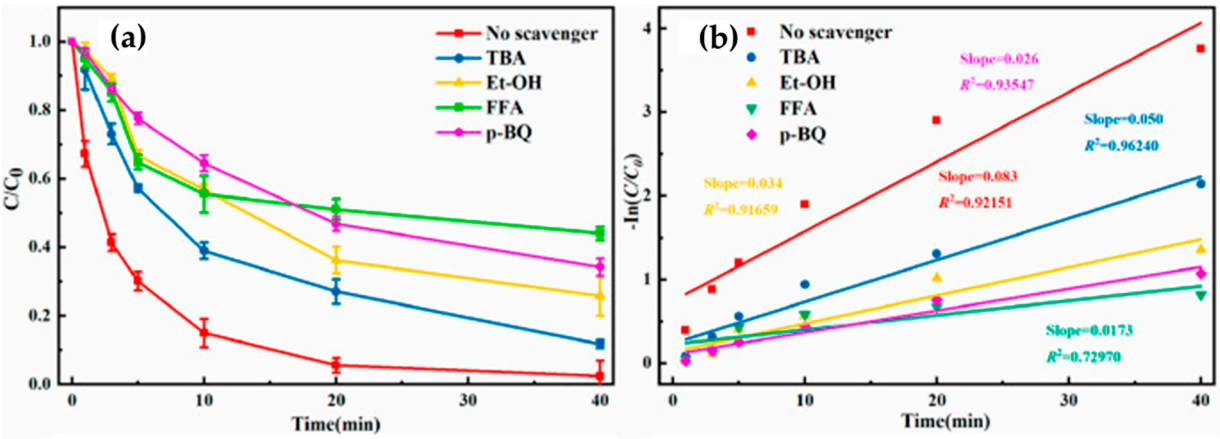

Figure 6. Example of (**a**) degradation spectra when quenching agents are added to determine the presence of the species and the effect they have on (**b**) the kinetic constants of the degradation process. Adapted from [148] copyright 2023 with permission from Elsevier (Amsterdam, The Netherlands).

The detection of the active species is governed by the reaction rate constant (K_{obs}) between the active species and the quenching agent (Table 3). Considering the radical mechanisms, methanol (MeOH) or ethanol (EtOH) is commonly used as a radical quencher to inhibit the contributions of both $HO^{\bullet}$ and $SO_4^{\bullet-}$ because of their reactivity with $SO_4^{\bullet-}$ [154,155]. Apparently, EtOH might be a more suitable quencher than MeOH to assess the relative contribution of $SO_4^{\bullet-}$ and $HO^{\bullet}$, as MeOH exhibits lower reactivity with $SO_4^{\bullet-}$. Additionally, Ghanbari and Moradi [156], in their literature review on the application and activation of PMS, also analyze this methodology for the identification of radicals. They explain that the difference in degradation efficiencies in the presence of MeOH or EtOH and TBA reflects the function of sulfate radicals. EtOH is commonly used

because, in various studies on contaminant degradation, the addition of EtOH showed a significant radical-scavenging effect, while the addition of TBA did not result in a significant quenching effect. This is because the α-hydrogen of EtOH can interact with $SO_4^{\bullet-}$ to generate • CHOH, which is capable of decomposing PMS [157]. TBA is usually employed as a radical scavenger to suppress the contribution of $HO^{\bullet}$ because it reacts faster with $HO^{\bullet}$ than with $SO_4^{\bullet-}$ [158,159]. Other chemical scavengers used such as furfuryl alcohol (FFA) [160,161], sodium azide (NaN_3) [162], and tryptophan [163,164] are typically adopted to recognize $^1O_2$. Nevertheless, it is important to mention that FFA can undergo a reaction with $HO^{\bullet}$, and NaN_3 can participate in a reaction with both $SO_4^{\bullet-}$ and $HO^{\bullet}$. Therefore, hindrance by FFA or NaN_3 can arise from their reactions not only with $^1O_2$ but also with $SO_4^{\bullet-}$ and $HO^{\bullet}$. Thus, the identified hindrance impact of FFA or NaN_3 is more significant than that of MeOH or EtOH but does not imply that $^1O_2$ is the predominant reactive species. Other chemical scavengers that react well with $HO^{\bullet}$ and $SO_4^{\bullet-}$ are employed, such as phenol [165], and potassium iodide is employed to pinpoint $SO_4^{\bullet-}$ and $HO^{\bullet}$ on the surface of materials. Para-benzoquinone (p-BQ) is utilized to recognize $O_2^{\bullet-}$ [166] and anisole [167].

Table 3. The rate constants of scavenging agents often employed with active species.

Scavenging Agents	Specific ROS	Kinetic Constants ($M^{-1}s^{-1}$)	Determination of ROS	Ref.
MeOH	$SO_4^{\bullet-}$ $HO^{\bullet}$	3.2×10^6 9.7×10^8	$SO_4^{\bullet-}$, $HO^{\bullet}$	[36]
EtOH	$SO_4^{\bullet-}$ $HO^{\bullet}$	$1.6–7.7 \times 10^7$ $1.2–2.8 \times 10^8$	$SO_4^{\bullet-}$, $HO^{\bullet}$	[155]
TBA	$SO_4^{\bullet-}$ $HO^{\bullet}$	$4–9.1 \times 10^5$ $3.8–7.6 \times 10^8$	$HO^{\bullet}$	[158]
p-BQ	$O_2^{\bullet-}$	1.0×10^9	$O_2^{\bullet-}$	[166]
FFA	$^1O_2$	3.2×10^7	$^1O_2$	[160]
NaN_3	$^1O_2$	1.2×10^8	$^1O_2$	[162]
Phenol	$SO_4^{\bullet-}$ $HO^{\bullet}$	8.8×10^9 6.6×10^9	$SO_4^{\bullet-}$, $HO^{\bullet}$	[165]

In general, if a chemical scavenger is stable, does not interfere with the catalysts, and exhibits significantly higher reactivity with $HO^{\bullet}$ and $SO_4^{\bullet-}$ in comparison with other oxidants present within the system, it can be utilized to remove or scavenge both $HO^{\bullet}$ and $SO_4^{\bullet-}$ species.

Overall, the combination of EPR/ESR and quenching experiments can effectively elucidate the existing active species, providing robust support for the activation of PMS. Consequently, when investigating the mechanism of activation during the reaction procedure, it is essential to integrate the active species identification methods of EPR and inhibition experiments to enhance the scientific rigor of the study.

4. Factors Influencing Reactivity

Various surrounding factors like the solution's pH value, PMS and catalyst concentrations, the existence of co-existing species, and the presence of natural organic matter (NOM) have an important influence on the activation of PMS via copper-based catalysts, further influencing the efficiency of organic substance removal.

4.1. Impact of pH on PMS Activation

The behavior of PMS is affected by the pH of the solution. Alkali conditions can activate the PMS. In acidic conditions (pH below 5), hydrogen ions operate as quenchers for $HO^{\bullet}$ and $SO_4^{\bullet-}$ [168,169]. Overall, PMS can be applied across a broad pH range. The

influence of pH across a broad spectrum (pH 3–11) on the activation of PMS through various Cu-based catalysts has been examined [93,170]. As an example, Mo et al. [170] investigated a pH range spanning from 3 to 11 and identified the most suitable pH as 6.5. The optimal pH values vary among different experiments ranging from pH 2 [171] to 5 [172] and to 11 [93]. There appears to be no consistent pattern regarding the effects of pH, possibly owing to the subsequent causes: Initially, a low pH leads to the dissolution and subsequent liberation of Cu^{2+} within the aqueous solution. In consequence, this could modify the surface structure of Cu-based materials, resulting in a reduction in reactivity. At low pH values, the abundance of protons could potentially challenge the Cu-based materials for PMS binding, thereby impeding the catalytic reactivity (Equations (10) and (11)).

$$SO_4^{\bullet -} + H^+ + e^- \rightarrow HSO_4^{\bullet -} \tag{10}$$

$$HO^{\bullet} + H^+ + e^- \rightarrow H_2O \tag{11}$$

Furthermore, the reactivity can be influenced by the catalytic interactions with PMS. Cu-based catalysts exhibit varying pHpzc (pH at the point of zero charge) values, leading to distinct surface charges at different pH levels. The variation in surface charges will influence the interaction between the Cu-based catalyst and PMS through electrostatic repulsion, consequently impacting the overall reactivity [173]. Thirdly, the transformation of radicals under different pH environments can lead to varying pH influences. The depletion of sulfate radicals can occur through their reaction with HO^-, bringing about the formation of hydroxyl-based radicals (Equation (1)) [174]. The redox potential of $HO^{\bullet}$ varies with pH, potentially affecting its reactivity.

As an example, the redox potential of $HO^{\bullet}$ has been observed to be 2.7 V in acidic solution but decreases to 1.8 V at neutral pH [175,176]. Moreover, the half-life of $SO_4^{\bullet -}$ is longer (30–40 µs) in water compared with that of the conventional $HO^{\bullet}$ ($10 - 3$ µs) [177]. Therefore, the transformation of $SO_4^{\bullet -}$ into $HO^{\bullet}$ could potentially impede the breakdown of contaminants at increased pH levels [178]. Managing the surface properties of Cu-based materials is essential for optimizing their efficiency within a broad pH range. The effect of pH on the activation of PMS by Cu-based catalysts is an important factor for optimizing the catalytic process and designing effective advanced oxidation systems for environmental remediation applications.

4.2. Impact of PMS and Catalyst Concentrations

The presence of PMS initiates the production of ROS, and varying PMS concentrations will result in distinct influences on the contaminant removal rate. Wang et al. [179] noted that the elimination rate of diethyl phthalate increased with rising PMS concentrations; however, it declined when the PMS concentration reached 5 mM. Additionally, Ji et al. [66] disclosed that the decolorization rate of RhB initially increased but later decreased with the rise in PMS concentration. The addition of PMS can increase the availability of oxidants, leading to enhanced degradation efficiency for pollutants. However, overabundant PMS can result in self-quenching reactions, which may be detrimental to the process. As depicted in the Equations (12) and (13), an excess of PMS will facilitate the transformation of $HO^{\bullet}$ and $SO_4^{\bullet -}$ into $SO_5^{\bullet -}$ and HSO_4^- with reduced reactivity [180,181]. Consequently, selecting the appropriate PMS concentration is of paramount importance for practical use [182].

$$HO^{\bullet} + HSO_5^- \rightarrow SO_5^{\bullet -} + H_2O \tag{12}$$

$$SO_4^{\bullet -} + HSO_5^- \rightarrow HSO_4^- + SO_5^{\bullet -} \tag{13}$$

The concentration of catalysts is also a crucial element in PMS activation. Raising the concentration of copper-based catalysts can not only introduce additional active sites for PMS activation but also enhance the likelihood of interacting with contaminant molecules. Furthermore, augmenting the concentration of copper-based catalysts proved advantageous in the production of radicals such as $SO_4^{\bullet -}$, which facilitated the elimination of

NPX [29]. However, an escalation in the concentration overabundant copper-based catalysts may produce an abundance of oxidative radicals and promote self-interaction amid radicals (Equations (14)–(16)) [183]. Yu et al. [184] observed that as the catalyst concentration rose from 0.1 g·L^{-1} to 0.3 g·L^{-1}, the removal rate of azo dye Orange G steadily rose. Nonetheless, it showed minimal change once the catalyst concentration surpassed 0.3 g·L^{-1}. The associated rationale may be that an excessive catalyst concentration leads to an overabundance of radical species, thereby raising the self-quenching rate of radicals.

$$HO^{\bullet} + HO^{\bullet} \rightarrow H_2O_2 \tag{14}$$

$$SO_4^{\bullet -} + SO_4^{\bullet -} \rightarrow S_2O_8 \tag{15}$$

$$SO_4^{\bullet -} + HO^{\bullet} \rightarrow HSO_5^{-} \tag{16}$$

According to Oh et al. [185], in the degradation process of BPA, increasing the PMS concentration has a lesser impact on BPA elimination compared to escalating the catalyst concentration. While raising the dose of PMS can indeed improve its reactivity and facilities the removal of pollutants, the limited active sites furnished by the catalyst will inevitably lead to competition among PMS molecules, which can influence the overall elimination procedure.

4.3. Anions

In Cu/PMS systems, anions such as Cl^-, HCO_3^-, PO_4^{3-}, and NO_3^- are able to interact with active oxidants, thereby impacting the efficiency of catalytic reactions. Chloride ions (Cl^-) are among the significant inorganic negatively charged ions present in water and in nearly all natural water sources [186]. On the other hand, $SO_4^{\bullet -}$, HSO_5^-, and $HO^{\bullet}$ possess the capability to oxidize Cl^- into less reactive chlorine or hypochlorous. For this reason, the existence of Cl^- in the systems demonstrates a restraining influence [187,188]. Researchers have clarified that the impeding influence of chloride is linked to the depletion of $SO_4^{\bullet -}$ and PMS in the process, which subsequently led to the generation of $Cl^{\bullet}$ and Cl_2, less active oxidizers [187,189]. This inhibitory effect can be succinctly illustrated in (Equations (17)–(21)).

$$SO_4^{\bullet -} + Cl^- \rightarrow SO_4^{2-} + Cl^{\bullet} \tag{17}$$

$$HSO_5^- + Cl^- \rightarrow SO_4^{2-} + HOCl \tag{18}$$

$$HSO_5^- + 2Cl^- + H^+ \rightarrow SO_4^{2-} + Cl_2 + H_2O \tag{19}$$

$$HO^{\bullet} + Cl^- \rightarrow HOCl^{\bullet -} \tag{20}$$

$$HOCl^{\bullet -} + H^+ \rightarrow Cl^{\bullet} + H_2O \tag{21}$$

Moreover, bicarbonate ion (HCO_3^-) is indeed one of the frequently encountered inorganic anions found in wastewater and water. It is formed by the combination of carbon dioxide (CO_2) and water (H_2O). According to research findings [190], HCO_3^- and dihydrogen phosphate ions ($H_2PO_4^-$) have a dual influence on the removal of pollutants. They can quench $SO_4^{\bullet -}$ and $HO^{\bullet}$ produced during the process and convert them into $HCO_3^{\bullet}$ and $H_2PO_4^{\bullet}$, respectively (Equations (22)–(24)).

$$HCO_3^- + SO_4^{\bullet -} \rightarrow SO_4^{2-} + CO_3^{\bullet -} + H^+ \tag{22}$$

$$HO^{\bullet} + HCO_3^- \rightarrow H_2O + CO_3^{\bullet -} \tag{23}$$

$$HO^{\bullet} + H_2PO_4^- \rightarrow HO^- + H_2PO_4^{\bullet} \tag{24}$$

However, the oxidation potential of $HCO_3^{\bullet}$ and $H_2PO_4^{\bullet}$ is less than that of $SO_4^{\bullet -}$ and $HO^{\bullet}$, which hinders the overall reaction [191,192]. A large concentration of HCO_3^- can adjust the system's pH to a basic environment around pH 8.5 [193]; this condition is

advantageous because it promotes the conversion of HSO_5^- to peroxymonosulfate (SO_5^{2-}), generating more opportunities for the generation of $^1O_2$ [92].

$$SO_4^{\bullet -} + H_2PO_4^- \rightarrow SO_4^{2-} + H_2PO_4^{\bullet} \quad (25)$$

Furthermore, the non-symmetric structure of PMS makes it susceptible to attack by nucleophiles like HCO_3^- and $H_2PO_4^-$, leading to rapid decomposition. As a result, HCO_3^- and $H_2PO_4^-$ can directly activate PMS [194]. Studies conducted by Du et al. [195] and Ye et al. [196] reported that $H_2PO_4^-$ and HCO_3^- have a beneficial impact on the elimination of pollutants. However, typically, $H_2PO_4^-$ and HCO_3^- still act as inhibitors, hindering the overall degradation process.

4.4. Natural Organic Matter

NOM is an omnipresent, intricate component found in natural aquatic environments and soils that can either boost or impede the breakdown of organic substances, contingent on the concentration and nature of NOM [197,198]. It has been noted that in certain instances, the interaction between NOM and $SO_4^{\bullet -}$ proceeds at a considerably slower pace compared to its interaction with $HO^{\bullet}$. This suggests that the presence of NOM might reduce the effectiveness of $SO_4^{\bullet -}$ in the removal of target contaminants [199]. Meanwhile, NOM can potentially initiate PMS activation, leading to the production of $SO_4^{\bullet -}$. This phenomenon arises from the creation of semiquinone radicals sourced from hydroquinones, quinones, and phenols present in NOM [92]. Nevertheless, NOM can also demonstrate adverse impacts. Typically, NOM functions as a scavenger of both $SO_4^{\bullet -}$ and $HO^{\bullet}$. It was observed that the breakdown effectiveness of ATZ using magnetic porous copper ferrite-catalyzed PMS decreased from 98% to 23% as the concentration of Suwannee River natural organic matter (SRNOM) increased from 0 to 3.2 mg·L^{-1} [92]. This decline happened due to the competitive interaction between SRNOM and ATZ for the accessible reactive radicals. Furthermore, the phenolic hydroxyl and carboxyl groups present in NOM can be adsorbed onto the surface of heterogeneous catalysts, obstructing the interaction of PMS with active sites [92]. Consequently, when implementing the Cu/PMS system, it becomes imperative to consider the influence of NOM.

5. Coupling Copper-Based Catalyst/PMS Systems with Other Advanced Oxidation Techniques

To form a combined AOP system, numerous AOPs, such as ozonation, ultrasonic irradiation, UV-Vis irradiation, and MW irradiation, have been integrated with copper-based catalyst/PMS systems. However, the intricacy of the reaction system increases with the addition of extra AOPs. On the other hand, the combined systems offer numerous potential benefits, including the synergistic improvement of organic contaminant degradation rates and improved PMS efficacy for pollutant elimination. Nevertheless, before incorporating further AOPs, two crucial factors need to be considered: first, the influence of incorporating additional AOPs on the catalyst's stability to prevent the early release of metal ions, and second, the additional treatment costs arising from the intricate setup, maintenance, and operation.

The amalgamated system that merges UV-Vis irradiation with a copper-based catalyst/PMS system has garnered the most extensive investigation. Diverse catalysts like copper nanoparticles [200], carbon-based Cu–Fe oxide [201], and $Co_{0.5}Cu_{0.5}Fe_2O_4$ magnetic nanoparticles [202] have been devised for activating PMS under UV-Vis irradiation. Generally, PMS can undergo activation through three feasible activation pathways in the copper-based catalyst/PMS/UV–Vis system: direct activation by UV irradiation, redox-based activation, and heterogeneous photocatalytic activation. While the combined impact appears to offer a hopeful outlook for future utilization, the advancement of the hybrid copper-based heterogeneous catalyst/PMS/UV–Vis system's catalyst is currently at an early stage. There remains a need for the creation of new catalysts to progress this field. It

is imperative for the catalyst to serve a dual function as both a photocatalyst and a PMS activator to effectively harness the collaborative influence.

The mixed configuration involving a disparate copper-based catalyst/PMS/ozone system has been the subject of prior examination, utilizing magnetic copper ferrite nanoparticles as the catalyst [203]. The introduction of ozone can augment the production of responsive radicals within the reaction environment, as ozone also has the capability to set PMS in motion, generating both $SO_4^{\bullet-}$ and $HO^{\bullet}$ [204]. A highly favorable condition is necessary to avert the self-scavenging reactions of different ROS.

Other combination systems using either ultrasonic [205] or MW [206] irradiation with copper-bases heterogeneous catalyst/PMS procedures have also been documented to yield a beneficial impact on the speed of contaminant elimination, attributed to the enhanced dynamics within the reaction environment. As an example, apart from expediting the cleansing of the catalyst's surface to enable redox reactions, US irradiation induces the formation of cavitation bubbles in the water. Upon their implosion, these bubbles lead to the creation of $SO_4^{\bullet-}$ and $HO^{\bullet}$ through the activation of PMS and the pyrolysis of water [207]. The MW irradiation raises the temperature of the water and generates localized high-temperature regions on the catalyst surface, thereby expediting the activation of PMS and facilitating faster redox reactions. Nevertheless, as the reactivity within the reaction system intensifies, it becomes crucial to consider the steadiness of the catalyst to avoid the untimely release of metal ions through dissolution.

6. Mechanisms for PMS Activation by Copper-Based Catalysts

The activation of PMS by Cu-based catalysts involves complex mechanisms that include both radical and non-radical pathways. The roles of catalysts are multifaceted, not only facilitating the formation of reactive species essential for pollutant degradation but also offering flexibility in choosing the appropriate pathway based on the nature of the pollutants and the desired outcomes. Understanding and leveraging these roles can lead to more efficient and targeted applications of Cu-based catalysts in environmental remediation. Understanding the distinct roles that Cu-based catalysts play in these pathways is crucial for optimizing their effectiveness in environmental remediation processes.

6.1. Radical Pathways

Copper-based catalysts trigger PMS to generate $SO_4^{\bullet-}$, $HO^{\bullet}$, and $O_2^{\bullet-}$ [29]. Considering their strong redox aptitude, $SO_4^{\bullet-}$, $HO^{\bullet}$, and $O_2^{\bullet-}$ could interact alongside specific contaminants and degrade them into lesser-sized molecules. Across most systems, $SO_4^{\bullet-}$ plays the key role as the active agent. To illustrate, Chen et al. [79] utilized a sol–gel combustion approach to synthesize a $CuFe_2O_4$ catalyst for triggering PMS. In the same research, TBA and EtOH were employed to inhibit $HO^{\bullet}$ and $SO_4^{\bullet-}$. The inhibitory effect of EtOH on TBBPA was significantly stronger compared to that on TBA. An EPR experiment showed DMPO-X's characteristic peak, pointing out that DMPO was oxidized by $SO_4^{\bullet-}$ and $HO^{\bullet}$. Consequently, the system was overshadowed by a $SO_4^{\bullet-}$-centered radical system. Feng et al. [95] fabricated $CuFeO_2$ rhombohedral crystals to initiate PMS activation for the disintegration of SDZ. EtOH and TBA were opted for as agents to counteract the presence of $SO_4^{\bullet-}$ and $HO^{\bullet}$ radicals. The results demonstrated that EtOH exhibited a higher inhibition effect on SDZ removal than TBA did, thereby affirming the prevalence of a radical mechanism primarily governed by $SO_4^{\bullet-}$. Furthermore, $HO^{\bullet}$ played a crucial function in certain systems, possibly influenced by the reaction pH or the specific characteristics of the specified substance [208]. Chi et al. [29] utilized ZVCu for the activation of PMS and the removal of NPX. DMPO-$SO_4^{\bullet-}$ and DMPO-$HO^{\bullet}$ signals were observed by ESR, and DMPO-$HO^{\bullet}$ signals were more intense than DMPO-$SO_4^{\bullet-}$ signals. To additionally illustrate the presence of active species, MeOH and TBA were utilized, and the suppression effect of TBA on NPX in the system was slightly less potent that of MeOH. Hence, the two radicals, $SO_4^{\bullet-}$ and $HO^{\bullet}$, in the ZVCu/PMS system participate in the removal reaction. Low-valent transition metal ions catalyze the activation of PMS to generate $SO_4^{\bullet-}$. Afterward, these radicals

react with H_2O or HO^- in the solution, resulting in the generation of $HO^\bullet$, which plays a primary role in the system. Nevertheless, quenching and EPR experiments cannot be used to investigate the presence of radicals in all PMS systems. In certain PMS systems, other approaches have been employed by some researchers to illustrate the reactive mechanism. A sol–gel method was utilized to synthesize a copper ferrate catalyst under the assumption of the sole existence of $HO^\bullet$ in the reaction system [92]. Hence, the elimination of nitrobenzene (NB) and ATZ by a $CuFe_2O_4$/PMS system was compared, and the contribution of $HO^\bullet$ on the catalyst surface was investigated according to the ratio of the quasi-first-order rate constant of reaction kinetics of each system during the degradation process. The results showed that the actual value of the ratio of quasi-first-order rate constants (k_{ATZ}/k_{NB} = 6.4) was much higher than the theoretical value (0.5~1), which proves that $SO_4^{\bullet-}$ and $HO^\bullet$ are the main active species on the catalyst surface.

A copper-based catalyst triggers the activation of PMS, leading to the formation of powerful radicals such as $SO_4^{\bullet-}$, $HO^\bullet$, and $O_2^{\bullet-}$. These radicals exhibit robust oxidative capabilities, enabling them to effectively target pollutants. The pollutants undergo degradation, breaking down into smaller molecules such as CO_2, inorganic oxides, and H_2O in a short time. Overall, the radical pathway proves to be a highly efficient approach for eliminating pollutants through AOPs.

6.2. Non-Radical Pathways

Nonetheless, in other PMS systems activated by copper-based catalysts, radicals have a limited role; in this case, the degradation of contaminants is primarily prompted by the non-radical route containing $^1O_2$ [209,210], electron transfer [211,212], and complexes. $^1O_2$ is a powerful ROS with high reactivity due to two electrons occupying the same energy level. It is effective in oxidizing organic pollutants. Generally, there exist three origins of production sources of $^1O_2$, involving the transformation of superoxide anion radicals (Equations (26)–(28)) [213].

$$O_2^{\bullet-} + HO^\bullet \rightarrow 1O_2 + OH^- \tag{26}$$

$$2O_2^{\bullet-} + 2H^+ \rightarrow H_2O_2 + 1O_2 \tag{27}$$

$$2O_2^{\bullet-} + 2H_2O \rightarrow 2OH^- + 1O_2 + H_2O_2 \tag{28}$$

The activation of PMS happens immediately (Equations (29) and (30)) [214–216]. Moreover, the transformation of functional groups occurs.

$$HSO_5^- \rightarrow SO_5^{2-} + H^+ \tag{29}$$

$$SO_5^{2-} + HSO_5^- \rightarrow O_2 + HSO_4^- + SO_4^{2-} \tag{30}$$

$^1O_2$ exhibits high selectivity in terms of the types of compounds it reacts with; electron-rich organic pollutants, like phenols, tend to be its target [217]. Understanding the selectivity of $^1O_2$ is crucial when designing and implementing oxidation processes for environmental remediation. It enables the development of tailored approaches for the efficient removal of specific pollutants while minimizing the impact on non-target compounds. Different types of catalyst materials based on copper can induce the generation of $^1O_2$ in PMS systems. For instance, copper-based catalysts containing graphite N (nitrogen) groups [218], as well as catalysts featuring C=O (carbonyl) groups, have been investigated. The carbonyl group, proposed as the active site on the aromatic ring, enhances PMS decomposition by forming a metastable dioxirane compound (*C-O-O-C*) as the crucial intermediate for $^1O_2$ formation. Additionally, magnetic catalysts with carbon-based carriers were studied [219]. All these catalysts facilitate the production of $^1O_2$ when they interact with PMS. The generation of $^1O_2$ provides an alternative non-radical pathway for pollutant removal in PMS systems.

Additionally, the pathway of electron transfer also contributes significantly to the removal of pollutants. In general, catalysts act as efficient electron transfer agents, trans-

ferring electrons from adsorbed hazardous substances to PMS, thereby enabling redox reactions [220].

Complex formation typically occurs on carbon-supported magnetic materials. That is, positively charged carbon creates a stable complex with significant redox capacity owing to the intense electrostatic attraction interacting with PMS (Equation (31)) [33,221].

$$Catalyst + PMS \rightarrow Catalyst - PMS^{*} \tag{31}$$

In contrast to the radical pathways, the activation mechanisms investigated in the subsequent systems are primarily initiated by the non-radical pathways. For instance, Li et al. [209] prepared a CuO-CeO_2 composite catalyst to activate PMS via an easy hydrothermal-calcination approach. In the degradation process of RhB, the authors found that $^1O_2$ was the dominant ROS in the CuO-CeO_2/PMS system. X-ray photoelectron microscopy analysis revealed that electron transfer occurred between CuO and CeO_2, along with the formation of oxygen vaccancies in CeO_2, which was responsible for enhancing the generation of $^1O_2$. This process introduces a new non-radical oxidation pathway for activating PMS using the CuO-CeO_2 catalyst. Pan et al. [212] developed a series of single-atom Cu embedded on porous N-doped biochar (SACu@NBC) as an economical catalyst to activate PMS to degrade large amounts of BPA. The presence of common radical scavengers did not hinder BPA elimination, indicating that radicals were not present. Experiments, such as quenching tests and scavenger degradation tests, ruled out the involvement of $^1O_2$. Ultimately, the dominant mechanism was identified as the electron transfer pathway in the SACu@NBC/PMS system via the anodizing analogy method that combined the quantitative structure–activity relationship. Moreover, dynamic fitting combined with density functional theory calculations revealed that the isolated atomic Cu in carbon supports acted as the active sites, narrowing the band gap and enhancing the electron transfer capacity. The catalyst-oxidation efficacy of SACu@NBC/PMS was effectively evidenced in an ultrafiltration device, indicating the potential of the electron transfer pathway in the SACu@NBC/PMS system aimed at elevated salinity effluent remediation.

PMS systems based AOPs are increasingly focusing on reformation due to the advantageous characteristics of non-radical pathways. These mechanisms can address certain constraints associated with radical activation, such as short half-lives. While the non-radical pathway does not primarily depend on vigorous oxidation to target pollutants (except for $^1O_2$), it does play a crucial role in facilitating redox reactions. This is achieved either by forming a complex with strong oxidation or through electron transfer within the reaction system, ultimately leading to the elimination of contaminants. It is crucial to emphasize that the non-radical pathway is not a singular process; rather, it may encompass two or more pathways. This complexity is essential to consider when examining the activation mechanism of PMS.

In addition to their capability to facilitate both radical and non-radical degradation pathways, Cu-based catalysts offer significant synergistic benefits through their dual pathway activation. Many Cu-based catalysts can activate PMS through both pathways simultaneously, resulting in enhanced degradation efficiency. This synergy allows different types of pollutants to be more effectively treated, as one pathway may be more suitable than the other for specific contaminants. For instance, $CuFe_2O_4$ catalysts are particularly versatile, participating in the generation of ROS via the radical pathway and the production of $^1O_2$ through the non-radical pathway, making them adaptable for various environmental applications.

Moreover, the catalytic activity of Cu-based catalysts can be finely tuned to favor one pathway over the other based on the specific requirements of the application. By adjusting parameters such as catalyst composition, surface modifications, and operating conditions like pH and temperature, it is possible to optimize the catalytic process. This not only maximizes pollutant degradation but also helps minimize secondary pollution and reduce energy consumption. These synergistic roles highlight the versatility and effec-

tiveness of Cu-based catalysts, further establishing them as key components in advanced environmental remediation technologies.

7. Toxicity Assessment after PMS-Based Processes

Toxicity is a vital parameter to be considered when studying the effectiveness of treatments to which wastewater has been subjected. In some cases, many intermediate products generated from pollutants present in treated water still possess strong biological toxicity and persistence in the environment, sometimes even greater than that of the original chemical, presenting a threat to human health and ecosystems [222,223]. Therefore, it is of great importance to evaluate the toxicity of effluents from treated waters, especially in cases where their possible reuse is considered.

There are numerous studies evaluating the toxicity of intermediate and by-products formed after PMS-based treatments [224–226]. Specifically analyzing those works in which Cu-based catalysts were used, it is found that a large number of authors have reported the relative toxicity calculated theoretically by applying Structure-Activity Ecological Relationship (ECOSAR) software (MS-Windows Version 2.2) [223,227]. The ECOSAR program evaluates the acute (LC_{50} and EC_{50}) and chronic (ChV) toxicity of compounds using three model aquatic organisms: fish, *Daphnia*, and *green algae*. The toxicity values obtained are classified into four groups: non-harmful ($LC_{50}/EC_{50}/ChV > 100$ mg/L), harmful (10 mg/L < $CL_{50}/EC_{50}/ChV < 100$ mg/L), toxic (1 mg/L < $LC_{50}/EC_{50}/ChV <$ 10 mg/L), and very toxic ($CL_{50}/EC_{50}/ChV < 1$ mg/L) [228,229]. Some PMS-based studies in which this software was used to determine the toxicity of the contaminant as well as that of the intermediate products obtained during the degradation process include the study of Mu et al. [230], where bisphenol A was treated with Cu^0-Fe_3O_4@Biochar; the work of Li et al. [231], in which the Orange G dye was degraded with carbon supporting CuCo nanospheres; the article of Liu et al. [232], where magnetic $CuFe_2O_4$ was prepared for the removal of oxytetracycline; and the study of Li et al. [233], where a newly compounded $ZnO/CuCo_2O_4$ was applied as a catalyst to decompose enrofloxacin under simulated sunlight. In all these studies, several degradation intermediates were identified, and their toxicity was evaluated using ECOSAR. In general, some of the generated intermediates were more toxic than the original pollutant, but the presence of these intermediates was very brief, as they decomposed almost immediately to yield other, non-harmful degradation products.

Moreover, a small number of articles evaluate toxicity using other techniques such as algal growth experiments, activated sludge inhibition tests, or bioluminescence tests. These tests are based on the direct assessment of the organism's inhibition of the treated solution to show its change in toxicity [228,229].

In the study conducted by Yan et al. [234], the potential toxicity of sulfamethoxazole and its intermediates after 60 min of treatment under a $CuO@Al_2O_3$(EPC)/PMS system using an activated sludge inhibition assay was evaluated. The results showed that the initial concentration of sulfamethoxazole (39.5 μM) produced a 42% inhibition in the oxygen absorption rate. In the first 20 min, the rate of oxygen absorption dropped sharply to 25%, and during the next 40 min, it gradually decreased to 16%. The results confirmed that the most toxic sulfamethoxazole was degraded into molecules of lower toxicity by the $CuO@Al_2O_3$ (EPC)/PMS system. In addition, the increased concentration of inorganic salts released during the degradation process (SO_4^{2-}, NO_3^-, NO_2^-, and NH_4^+) confirmed high mineralization.

In the study of Huang et al. [235], the acute toxicity of arsanilic acid and its oxidation by-products were evaluated by the bioluminescence of the marine bacterium *Vibrio fischeri*. The results showed that the initial arsanilic acid inhibition ratio (26.72 μM) was approximately 6.8%; the inhibition ratio increased rapidly to 46.4% after 40 min of reaction and then slightly decreased. As the reaction developed, the arsanilic acid rapidly degraded to release aromatic compounds and inorganic arsenic, resulting in a rapid increase in toxicity of the reaction solution. Meanwhile, these released products were partially eliminated due to adsorption and mineralization by the $CuFe_2O_4$/PMS system, slightly decreasing toxicity.

In this case, the intermediate compounds were more toxic than the original ones; therefore, it would be necessary to develop other technologies combined with the $CuFe_2O_4$/PMS system to reduce residual toxicity.

In conclusion, most of the reviewed studies indicate that treated water is generally non-toxic, suggesting that PMS-based degradation processes with Cu catalysts are effective. However, in cases where toxicity persists, it may be necessary to combine additional treatment systems with PMS-based processes to completely eliminate residual toxicity.

8. Conclusions and Outlooks

In conclusion, a wide variety of copper-based catalysts can be considered for PMS activation, with particular attention to emerging materials such as MOFs, LDHs, and DESs. These materials offer promising avenues for the development of advanced catalysts, as they provide enhanced stability, increased surface area, and tunable properties. These characteristics make them excellent candidates for improving the efficiency and selectivity of catalytic processes in environmental applications.

As demonstrated throughout this study, the activation of PMS by copper-based catalysts has yielded promising results in the treatment of persistent pollutants in wastewater. Cu-based catalysts exhibit remarkable versatility in both radical and non-radical pathways, offering significant advantages across various environmental conditions. Their ability to efficiently generate ROS, such as sulfate radicals and hydroxyl radicals, as well as singlet oxygen through non-radical pathways, underscores their potential in diverse applications. Furthermore, the use of these catalysts provides an economically viable and environmentally sustainable solution for water treatment. Utilizing these catalysts in heterogeneous forms, which reduces secondary pollution from copper ion leaching, further enhances their practical applicability. Additionally, water treated through PMS-based degradation processes, particularly with Cu catalysts, is generally found to be non-toxic, reinforcing the effectiveness of these methods. However, as with any treatment process, when residual toxicity remains, it may be necessary to integrate additional treatment systems with the PMS-based processes to ensure the elimination of any lingering toxic compounds.

Despite the high effectiveness of Cu-based catalysts, challenges such as metal leaching and the need for optimized catalyst design must be addressed. Certain limitations still exist, and further research is required to unlock the full potential of these catalysts. The main outlooks for future work include the following:

- Future research directions: Continued research should focus on enhancing the stability and reusability of Cu-based catalysts, particularly through innovative catalyst design and the exploration of new materials such as bimetallic MOFs and advanced LDHs. Further investigation into the mechanisms of PMS activation, especially under real-world conditions, will be critical for optimizing these systems.
- Real applications: The translation of laboratory findings into large-scale industrial applications remains a key objective. This includes scaling up the synthesis of Cu-based catalysts and integrating them into existing wastewater treatment infrastructure. The potential for coupling Cu-based catalysts with other AOPs offers exciting opportunities for developing more efficient and comprehensive treatment systems.
- Sustainability considerations: As environmental regulations become more stringent, the demand for sustainable water treatment technologies will continue to grow. Cu-based catalysts, with their low toxicity and high efficiency, are well-positioned to meet this demand. Future developments should prioritize minimizing the environmental footprint of these catalysts, ensuring they contribute to a circular economy by enabling the recovery and reuse of resources.

In summary, Cu-based catalysts represent a promising and versatile tool in the fight against water pollution. Their ability to activate PMS and degrade a wide range of organic pollutants positions them as a key component of modern wastewater treatment strategies. However, achieving their full potential will require ongoing research, innovation, and a commitment to sustainability. By addressing current challenges and exploring new avenues

for catalyst development, Cu-based systems can play a pivotal role in creating cleaner and safer water resources for the future.

Author Contributions: Conceptualization, B.B. and M.Á.S.; resources, M.Á.S.; writing—original draft preparation, B.B., B.L.-F. and A.F.-S.; writing—review and editing, S.C.E. and M.Á.S.; visualization, B.B., A.F.-S. and M.Á.S.; supervision, M.Á.S.; project administration, M.Á.S.; funding acquisition, M.Á.S. All authors have read and agreed to the published version of the manuscript.

Funding: This research has been supported by R&D Project PCI2022-132941 funded by MICIU/AEI/10.13039/501100011033 and by the European Union Next Generation EU/PRTR. Xunta de Galicia and European Regional Development Fund for their support in project ED431C 2021-43. R&D Project PID2020-113667 GB-I00 funded by MICIU/AEI/10.13039/501100011033. Also, Antía Fdez-Sanromán thanks MICIU/AEI/10.13039/501100011033 and FSE+ investing in your future for her predoctoral fellowship (PRE2021-098540).

Data Availability Statement: Not applicable.

Conflicts of Interest: The authors declare no conflicts of interest.

References

1. Manzoor, M.H.; Naz, N.; Naqvi, S.M.G.; Ashraf, S.; Ashiq, M.Z.; Verpoort, F. Wastewater Treatment Using Metal-Organic Frameworks (MOFs). *Appl. Mater. Today* **2024**, *40*, 102358. [CrossRef]
2. Alayande, A.B.; Qi, W.; Karthikeyan, R.; Popat, S.C.; Ladner, D.A.; Amy, G. Use of Reclaimed Municipal Wastewater in Agriculture: Comparison of Present Practice versus an Emerging Paradigm of Anaerobic Membrane Bioreactor Treatment Coupled with Hydroponic Controlled Environment Agriculture. *Water Res.* **2024**, *265*, 122197. [CrossRef]
3. Lincho, J.; Martins, R.C.; Gomes, J. Paraben Compounds—Part I: An Overview of Their Characteristics, Detection, and Impacts. *Appl. Sci.* **2021**, *11*, 2307. [CrossRef]
4. Kumar, R.; Qureshi, M.; Vishwakarma, D.K.; Al-Ansari, N.; Kuriqi, A.; Elbeltagi, A.; Saraswat, A. A Review on Emerging Water Contaminants and the Application of Sustainable Removal Technologies. *Case Stud. Chem. Environ. Eng.* **2022**, *6*, 100219. [CrossRef]
5. Silva, S.; Cardoso, V.V.; Duarte, L.; Carneiro, R.N.; Almeida, C.M.M. Characterization of Five Portuguese Wastewater Treatment Plants: Removal Efficiency of Pharmaceutical Active Compounds through Conventional Treatment Processes and Environmental Risk. *Appl. Sci.* **2021**, *11*, 7388. [CrossRef]
6. Pandey, P.K.; Kass, P.H.; Soupir, M.L.; Biswas, S.; Singh, V.P. Contamination of Water Resources by Pathogenic Bacteria. *AMB Express* **2014**, *4*, 51. [CrossRef] [PubMed]
7. Hazra, M.; Joshi, H.; Williams, J.B.; Watts, J.E.M. Antibiotics and Antibiotic Resistant Bacteria/Genes in Urban Wastewater: A Comparison of Their Fate in Conventional Treatment Systems and Constructed Wetlands. *Chemosphere* **2022**, *303*, 135148. [CrossRef]
8. Mary Ealias, A.; Meda, G.; Tanzil, K. Recent Progress in Sustainable Treatment Technologies for the Removal of Emerging Contaminants from Wastewater: A Review on Occurrence, Global Status and Impact on Biota. *Rev. Environ. Contam. Toxicol.* **2024**, *262*, 16. [CrossRef]
9. Hassani, A.; Scaria, J.; Ghanbari, F.; Nidheesh, P. V Sulfate Radicals-Based Advanced Oxidation Processes for the Degradation of Pharmaceuticals and Personal Care Products: A Review on Relevant Activation Mechanisms, Performance, and Perspectives. *Environ. Res.* **2023**, *217*, 114789. [CrossRef]
10. Pisharody, L.; Gopinath, A.; Malhotra, M.; Nidheesh, P.V.; Kumar, M.S. Occurrence of Organic Micropollutants in Municipal Landfill Leachate and Its Effective Treatment by Advanced Oxidation Processes. *Chemosphere* **2022**, *287*, 132216. [CrossRef]
11. Sandoval, M.A.; Vidal, J.; Calzadilla, W.; Salazar, R. Solar (Electrochemical) Advanced Oxidation Processes as Efficient Treatments for Degradation of Pesticides. *Curr. Opin. Electrochem.* **2022**, *36*, 101125. [CrossRef]
12. Ike, I.A.; Linden, K.G.; Orbell, J.D.; Duke, M. Critical Review of the Science and Sustainability of Persulphate Advanced Oxidation Processes. *Chem. Eng. J.* **2018**, *338*, 651–669. [CrossRef]
13. Wang, J.; Wang, S. Activation of Persulfate (PS) and Peroxymonosulfate (PMS) and Application for the Degradation of Emerging Contaminants. *Chem. Eng. J.* **2018**, *334*, 1502–1517. [CrossRef]
14. Liu, G.; Li, C.; Stewart, B.A.; Liu, L.; Zhang, M.; Yang, M.; Lin, K. Enhanced Thermal Activation of Peroxymonosulfate by Activated Carbon for Efficient Removal of Perfluorooctanoic Acid. *Chem. Eng. J.* **2020**, *399*, 125722. [CrossRef]
15. Mahdi-Ahmed, M.; Chiron, S. Ciprofloxacin Oxidation by UV-C Activated Peroxymonosulfate in Wastewater. *J. Hazard. Mater.* **2014**, *265*, 41–46. [CrossRef]
16. Long, M.; Li, D.; Li, H.; Ma, X.; Zhao, Q.; Wen, Q.; Song, F. Synergetic Effect of Photocatalysis and Peroxymonosulfate Activated by MFe_2O_4 (M = Co, Mn, or Zn) for Enhanced Photocatalytic Activity under Visible Light Irradiation. *RSC Adv.* **2022**, *12*, 20946–20955. [CrossRef]

17. Fu, J.; Feng, L.; Liu, Y.; Zhang, L.; Li, S. Electrochemical Activation of Peroxymonosulfate (PMS) by Carbon Cloth Anode for Sulfamethoxazole Degradation. *Chemosphere* **2022**, *287*, 132094. [CrossRef] [PubMed]
18. Yin, R.; Guo, W.; Wang, H.; Du, J.; Zhou, X.; Wu, Q.; Zheng, H.; Chang, J.; Ren, N. Enhanced Peroxymonosulfate Activation for Sulfamethazine Degradation by Ultrasound Irradiation: Performances and Mechanisms. *Chem. Eng. J.* **2018**, *335*, 145–153. [CrossRef]
19. Bouzayani, B.; Rosales, E.; Pazos, M.; Elaoud, S.C.; Sanromán, M.A. Homogeneous and Heterogeneous Peroxymonosulfate Activation by Transition Metals for the Degradation of Industrial Leather Dye. *J. Clean. Prod.* **2019**, *228*, 222–230. [CrossRef]
20. Oh, W.-D.; Dong, Z.; Lim, T.-T. Generation of Sulfate Radical through Heterogeneous Catalysis for Organic Contaminants Removal: Current Development, Challenges and Prospects. *Appl. Catal. B* **2016**, *194*, 169–201. [CrossRef]
21. Hu, J.; Zou, Y.; Li, Y.; Xiao, Y.; Li, M.; Lin, L.; Li, B.; Li, X. Efficacy and Mechanism of Peroxymonosulfate Activation by Single-Atom Transition Metal Catalysts for the Oxidation of Organic Pollutants: Experimental Validation and Theoretical Calculation. *J. Colloid Interface Sci.* **2023**, *645*, 1–11. [CrossRef] [PubMed]
22. Liu, T.; Yin, K.; Li, N.; Liu, H.; Chen, J.; Zhou, X.; Zhang, Y. Efficient Activation of Peroxymonosulfate by Copper Supported on Polyurethane Foam for Contaminant Degradation: Synergistic Effect and Mechanism. *Chem. Eng. J.* **2022**, *427*, 131741. [CrossRef]
23. Guo, S.; Chen, M.; You, L.; Wei, Y.; Cai, C.; Wei, Q.; Zhang, H.; Zhou, K. 3D Printed Hierarchically Porous Zero-Valent Copper for Efficient Pollutant Degradation through Peroxymonosulfate Activation. *Sep. Purif. Technol.* **2023**, *305*, 122437. [CrossRef]
24. Singh, S.; Patidar, R.; Srivastava, V.C.; Kumar, P.; Singh, A.; Lo, S.-L. Ellipsoid-Shaped Copper Oxide as an Effective Peroxymonosulfate Activator for Perfluorooctanoic Acid Decomposition. *Mater. Today Commun.* **2023**, *34*, 105107. [CrossRef]
25. Zuo, X.; Jiang, A.; Zou, S.; Wu, J.; Ding, B. Copper Oxides Activate Peroxymonosulfate for Degradation of Methylene Blue via Radical and Nonradical Pathways: Surface Structure and Mechanism. *Environ. Sci. Pollut. Res.* **2023**, *30*, 13023–13038. [CrossRef]
26. Wang, C.; Dai, H.; Liang, L.; Li, N.; Cui, X.; Yan, B.; Chen, G. Enhanced Mechanism of Copper Doping in Magnetic Biochar for Peroxymonosulfate Activation and Sulfamethoxazole Degradation. *J. Hazard. Mater.* **2023**, *458*, 132002. [CrossRef] [PubMed]
27. Zhou, P.; Liu, B.; Zhang, J.; Zhang, Y.; Zhang, G.; Wei, C.; Liang, J.; Liu, Y.; Zhang, W. Radicals Induced from Peroxomonosulfate by Nanoscale Zero-Valent Copper in the Acidic Solution. *Water Sci. Technol.* **2016**, *74*, 1946–1952. [CrossRef] [PubMed]
28. Zhou, P.; Zhang, J.; Zhang, Y.; Zhang, G.; Li, W.; Wei, C.; Liang, J.; Liu, Y.; Shu, S. Degradation of 2,4-Dichlorophenol by Activating Persulfate and Peroxomonosulfate Using Micron or Nanoscale Zero-Valent Copper. *J. Hazard. Mater.* **2018**, *344*, 1209–1219. [CrossRef]
29. Chi, H.; Wang, Z.; He, X.; Zhang, J.; Wang, D.; Ma, J. Activation of Peroxymonosulfate System by Copper-Based Catalyst for Degradation of Naproxen: Mechanisms and Pathways. *Chemosphere* **2019**, *228*, 54–64. [CrossRef]
30. Hu, J.; Dong, H.; Qu, J.; Qiang, Z. Enhanced Degradation of Iopamidol by Peroxymonosulfate Catalyzed by Two Pipe Corrosion Products (CuO and δ-MnO_2). *Water Res.* **2017**, *112*, 1–8. [CrossRef]
31. Du, X.; Zhang, Y.; Si, F.; Yao, C.; Du, M.; Hussain, I.; Kim, H.; Huang, S.; Lin, Z.; Hayat, W. Persulfate Non-Radical Activation by Nano-CuO for Efficient Removal of Chlorinated Organic Compounds: Reduced Graphene Oxide-Assisted and CuO (0 0 1) Facet-Dependent. *Chem. Eng. J.* **2019**, *356*, 178–189. [CrossRef]
32. Wang, S.; Gao, S.; Tian, J.; Wang, Q.; Wang, T.; Hao, X.; Cui, F. A Stable and Easily Prepared Copper Oxide Catalyst for Degradation of Organic Pollutants by Peroxymonosulfate Activation. *J. Hazard. Mater.* **2020**, *387*, 121995. [CrossRef] [PubMed]
33. Li, H.; Tian, J.; Xiao, F.; Huang, R.; Gao, S.; Cui, F.; Wang, S.; Duan, X. Structure-Dependent Catalysis of Cuprous Oxides in Peroxymonosulfate Activation via Nonradical Pathway with a High Oxidation Capacity. *J. Hazard. Mater.* **2020**, *385*, 121518. [CrossRef]
34. Li, G.; Zhong, Z.; Yang, C.; He, Q.; Peng, G. Degradation of Acid Orange 7 by Peroxymonosulfate Activated by Cupric Oxide. *J. Water Supply Res. Technol.—AQUA* **2019**, *68*, 29–38. [CrossRef]
35. Qin, Q.; Qiao, N.; Liu, Y.; Wu, X. Spongelike Porous CuO as an Efficient Peroxymonosulfate Activator for Degradation of Acid Orange 7. *Appl. Surf. Sci.* **2020**, *521*, 146479. [CrossRef]
36. Xu, Y.; Ai, J.; Zhang, H. The Mechanism of Degradation of Bisphenol A Using the Magnetically Separable $CuFe_2O_4$/Peroxymonosulfate Heterogeneous Oxidation Process. *J. Hazard. Mater.* **2016**, *309*, 87–96. [CrossRef]
37. Ding, Y.; Zhu, L.; Wang, N.; Tang, H. Sulfate Radicals Induced Degradation of Tetrabromobisphenol A with Nanoscaled Magnetic $CuFe_2O_4$ as a Heterogeneous Catalyst of Peroxymonosulfate. *Appl. Catal. B* **2013**, *129*, 153–162. [CrossRef]
38. Selvan, R.K.; Augustin, C.O.; Berchmans, L.J.; Saraswathi, R. Combustion Synthesis of $CuFe_2O_4$. *Mater. Res. Bull.* **2003**, *38*, 41–54. [CrossRef]
39. Wang, Y.; Tian, D.; Chu, W.; Li, M.; Lu, X. Nanoscaled Magnetic $CuFe_2O_4$ as an Activator of Peroxymonosulfate for the Degradation of Antibiotics Norfloxacin. *Sep. Purif. Technol.* **2019**, *212*, 536–544. [CrossRef]
40. Kiani, R.; Mirzaei, F.; Ghanbari, F.; Feizi, R.; Mehdipour, F. Real Textile Wastewater Treatment by a Sulfate Radicals-Advanced Oxidation Process: Peroxydisulfate Decomposition Using Copper Oxide (CuO) Supported onto Activated Carbon. *J. Water Process Eng.* **2020**, *38*, 101623. [CrossRef]
41. Ren, Y.; Lin, L.; Ma, J.; Yang, J.; Feng, J.; Fan, Z. Sulfate Radicals Induced from Peroxymonosulfate by Magnetic Ferrospinel MFe_2O_4 (M = Co, Cu, Mn, and Zn) as Heterogeneous Catalysts in the Water. *Appl. Catal. B* **2015**, *165*, 572–578. [CrossRef]
42. Wang, R.; An, H.; Zhang, H.; Zhang, X.; Feng, J.; Wei, T.; Ren, Y. High Active Radicals Induced from Peroxymonosulfate by Mixed Crystal Types of $CuFeO_2$ as Catalysts in the Water. *Appl. Surf. Sci.* **2019**, *484*, 1118–1127. [CrossRef]

43. Fang, Y.; Guo, Y. Copper-Based Non-Precious Metal Heterogeneous Catalysts for Environmental Remediation. *Chin. J. Catal.* **2018**, *39*, 566–582. [CrossRef]
44. Aflak, N.; Ben El Ayouchia, H.; Bahsis, L.; Anane, H.; Julve, M.; Stiriba, S.-E. Recent Advances in Copper-Based Solid Heterogeneous Catalysts for Azide–Alkyne Cycloaddition Reactions. *Int. J. Mol. Sci.* **2022**, *23*, 2383. [CrossRef] [PubMed]
45. Zheng, X.; Niu, X.; Zhang, D.; Lv, M.; Ye, X.; Ma, J.; Lin, Z.; Fu, M. Metal-Based Catalysts for Persulfate and Peroxymonosulfate Activation in Heterogeneous Ways: A Review. *Chem. Eng. J.* **2022**, *429*, 132323. [CrossRef]
46. Yang, L.; Ren, X.; Zhang, Y.; Chen, Z. One-Pot Preparation of Poly (Triazine Imide) with Intercalation of Cu Ions: A Heterogeneous Catalyst for Peroxymonosulfate Activation to Degradate Organic Pollutants under Sunlight. *Inorg. Chem. Commun.* **2022**, *145*, 109965. [CrossRef]
47. Fu, C.; Yan, M.; Ma, H.; Zhang, S.; Yang, G.; Tian, H.; Yang, J.; Wang, Z.; Zhu, S.; Bhatt, K.; et al. Synthetic Organic Compounds Degradation by Dual Radical/Non-Radical Peroxymonosulfate with Copper Oxide as Efficient Heterogeneous Activator. *J. Taiwan Inst. Chem. Eng.* **2023**, *146*, 104839. [CrossRef]
48. Zhu, Q.; Zhang, M.; Ma, Q. Copper-Based Foliar Fertilizer and Controlled Release Urea Improved Soil Chemical Properties, Plant Growth and Yield of Tomato. *Sci. Hortic.* **2012**, *143*, 109–114. [CrossRef]
49. Yong, S.T.; Ooi, C.W.; Chai, S.-P.; Wu, X.S. Review of Methanol Reforming-Cu-Based Catalysts, Surface Reaction Mechanisms, and Reaction Schemes. *Int. J. Hydrogen Energy* **2013**, *38*, 9541–9552. [CrossRef]
50. Borkow, G.; Gabbay, J. Copper, an Ancient Remedy Returning to Fight Microbial, Fungal and Viral Infections. *Curr. Chem. Biol.* **2009**, *3*, 272–278.
51. Khalaj, M.; Kamali, M.; Khodaparast, Z.; Jahanshahi, A. Copper-Based Nanomaterials for Environmental Decontamination—An Overview on Technical and Toxicological Aspects. *Ecotoxicol. Environ. Saf.* **2018**, *148*, 813–824. [CrossRef]
52. Fu, F.; Dionysiou, D.D.; Liu, H. The Use of Zero-Valent Iron for Groundwater Remediation and Wastewater Treatment: A Review. *J. Hazard. Mater.* **2014**, *267*, 194–205. [CrossRef] [PubMed]
53. Zhang, Y.; Fan, J.; Yang, B.; Huang, W.; Ma, L. Copper–Catalyzed Activation of Molecular Oxygen for Oxidative Destruction of Acetaminophen: The Mechanism and Superoxide-Mediated Cycling of Copper Species. *Chemosphere* **2017**, *166*, 89–95. [CrossRef] [PubMed]
54. Nidheesh, P.V.; Khatri, J.; Singh, T.S.A.; Gandhimathi, R.; Ramesh, S.T. Review of Zero-Valent Aluminium Based Water and Wastewater Treatment Methods. *Chemosphere* **2018**, *200*, 621–631. [CrossRef] [PubMed]
55. O'Carroll, D.; Sleep, B.; Krol, M.; Boparai, H.; Kocur, C. Nanoscale Zero Valent Iron and Bimetallic Particles for Contaminated Site Remediation. *Adv. Water Resour.* **2013**, *51*, 104–122. [CrossRef]
56. Yamaguchi, R.; Kurosu, S.; Suzuki, M.; Kawase, Y. Hydroxyl Radical Generation by Zero-Valent Iron/Cu (ZVI/Cu) Bimetallic Catalyst in Wastewater Treatment: Heterogeneous Fenton/Fenton-like Reactions by Fenton Reagents Formed in-Situ under Oxic Conditions. *Chem. Eng. J.* **2018**, *334*, 1537–1549. [CrossRef]
57. Kohantorabi, M.; Moussavi, G.; Giannakis, S. A Review of the Innovations in Metal-and Carbon-Based Catalysts Explored for Heterogeneous Peroxymonosulfate (PMS) Activation, with Focus on Radical vs. Non-Radical Degradation Pathways of Organic Contaminants. *Chem. Eng. J.* **2021**, *411*, 127957. [CrossRef]
58. Oh, W.-D.; Zaeni, J.R.J.; Lisak, G.; Lin, K.-Y.A.; Leong, K.-H.; Choong, Z.-Y. Accelerated Organics Degradation by Peroxymonosulfate Activated with Biochar Co-Doped with Nitrogen and Sulfur. *Chemosphere* **2021**, *277*, 130313. [CrossRef]
59. de Sousa, P.V.F.; de Oliveira, A.F.; da Silva, A.A.; Lopes, R.P. Environmental Remediation Processes by Zero Valence Copper: Reaction Mechanisms. *Environ. Sci. Pollut. Res.* **2019**, *26*, 14883–14903. [CrossRef]
60. Zhang, T.; Yang, Y.; Li, X.; Yu, H.; Wang, N.; Li, H.; Du, P.; Jiang, Y.; Fan, X.; Zhou, Z. Degradation of Sulfamethazine by Persulfate Activated with Nanosized Zero-Valent Copper in Combination with Ultrasonic Irradiation. *Sep. Purif. Technol.* **2020**, *239*, 116537. [CrossRef]
61. Deng, Y.; Zhao, R. Advanced Oxidation Processes (AOPs) in Wastewater Treatment. *Curr. Pollut. Rep.* **2015**, *1*, 167–176. [CrossRef]
62. Zhou, P.; Zhang, J.; Liu, J.; Zhang, Y.; Liang, J.; Liu, Y.; Liu, B.; Zhang, W. Degradation of Organic Contaminants by Activated Persulfate Using Zero Valent Copper in Acidic Aqueous Conditions. *RSC Adv.* **2016**, *6*, 99532–99539. [CrossRef]
63. Feng, Y.; Wu, D.; Liao, C.; Deng, Y.; Zhang, T.; Shih, K. Red Mud Powders as Low-Cost and Efficient Catalysts for Persulfate Activation: Pathways and Reusability of Mineralizing Sulfadiazine. *Sep. Purif. Technol.* **2016**, *167*, 136–145. [CrossRef]
64. Matzek, L.W.; Carter, K.E. Activated Persulfate for Organic Chemical Degradation: A Review. *Chemosphere* **2016**, *151*, 178–188. [CrossRef]
65. Ghanbari, F.; Moradi, M.; Manshouri, M. Textile Wastewater Decolorization by Zero Valent Iron Activated Peroxymonosulfate: Compared with Zero Valent Copper. *J. Environ. Chem. Eng.* **2014**, *2*, 1846–1851. [CrossRef]
66. Ji, F.; Li, C.; Liu, Y.; Liu, P. Heterogeneous Activation of Peroxymonosulfate by Cu/ZSM5 for Decolorization of Rhodamine B. *Sep. Purif. Technol.* **2014**, *135*, 1–6. [CrossRef]
67. Zhang, Q.; Zhang, K.; Xu, D.; Yang, G.; Huang, H.; Nie, F.; Liu, C.; Yang, S. CuO Nanostructures: Synthesis, Characterization, Growth Mechanisms, Fundamental Properties, and Applications. *Prog. Mater. Sci.* **2014**, *60*, 208–337. [CrossRef]
68. Ghanbari, F.; Jaafarzadeh, N. Graphite-Supported CuO Catalyst for Heterogeneous Peroxymonosulfate Activation to Oxidize Direct Orange 26: The Effect of Influential Parameters. *Res. Chem. Intermed.* **2017**, *43*, 4623–4637. [CrossRef]
69. Chen, L.; Li, L.; Li, G. Synthesis of CuO Nanorods and Their Catalytic Activity in the Thermal Decomposition of Ammonium Perchlorate. *J. Alloys Compd.* **2008**, *464*, 532–536. [CrossRef]

70. Oha, W.-D.; Luaa, S.-K.; Donga, Z.; Lima, T.-T. A Novel Three-Dimensional Spherical $CuBi_2O_4$ Nanocolumn Arrays with Persulfate and Peroxymonosulfate Activation Functionalities for 1*H*-Benzotriazole Removal. *Nanoscale* **2015**, *7*, 8149–8158. [CrossRef]
71. Feng, Y.; Liu, J.; Wu, D.; Zhou, Z.; Deng, Y.; Zhang, T.; Shih, K. Efficient Degradation of Sulfamethazine with $CuCo_2O_4$ Spinel Nanocatalysts for Peroxymonosulfate Activation. *Chem. Eng. J.* **2015**, *280*, 514–524. [CrossRef]
72. Ji, F.; Li, C.; Deng, L. Performance of CuO/Oxone System: Heterogeneous Catalytic Oxidation of Phenol at Ambient Conditions. *Chem. Eng. J.* **2011**, *178*, 239–243. [CrossRef]
73. Zhang, T.; Zhu, H.; Croue, J.-P. Production of Sulfate Radical from Peroxymonosulfate Induced by a Magnetically Separable $CuFe_2O_4$ Spinel in Water: Efficiency, Stability, and Mechanism. *Environ. Sci. Technol.* **2013**, *47*, 2784–2791. [CrossRef]
74. Kušić, H.; Koprivanac, N.; Selanec, I. Fe-Exchanged Zeolite as the Effective Heterogeneous Fenton-Type Catalyst for the Organic Pollutant Minimization: UV Irradiation Assistance. *Chemosphere* **2006**, *65*, 65–73. [CrossRef]
75. Liu, J.; Jiang, G.; Liu, Y.; Di, J.; Wang, Y.; Zhao, Z.; Sun, Q.; Xu, C.; Gao, J.; Duan, A.; et al. Hierarchical Macro-Meso-Microporous ZSM-5 Zeolite Hollow Fibers with Highly Efficient Catalytic Cracking Capability. *Sci. Rep.* **2014**, *4*, 7276. [CrossRef]
76. Yang, Z.; Dai, D.; Yao, Y.; Chen, L.; Liu, Q.; Luo, L. Extremely Enhanced Generation of Reactive Oxygen Species for Oxidation of Pollutants from Peroxymonosulfate Induced by a Supported Copper Oxide Catalyst. *Chem. Eng. J.* **2017**, *322*, 546–555. [CrossRef]
77. Zhu, X.; Zhang, Y.; Yan, W.; Yang, S.; Wu, K.; Wang, G.; Jin, P.; Wei, J. Peroxymonosulfate Activation by Mesoporous CuO Nanocage for Organic Pollutants Degradation via a Singlet Oxygen-Dominated Pathway. *J. Environ. Chem. Eng.* **2021**, *9*, 106757. [CrossRef]
78. Li, Z.; Liu, D.; Huang, W.; Wei, X.; Huang, W. Biochar Supported CuO Composites Used as an Efficient Peroxymonosulfate Activator for Highly Saline Organic Wastewater Treatment. *Sci. Total Environ.* **2020**, *721*, 137764. [CrossRef]
79. Chen, Z.; Wang, L.; Xu, H.; Wen, Q. Efficient Heterogeneous Activation of Peroxymonosulfate by Modified $CuFe_2O_4$ for Degradation of Tetrabromobisphenol A. *Chem. Eng. J.* **2020**, *389*, 124345. [CrossRef]
80. Rodríguez-Chueca, J.; Barahona-García, E.; Blanco-Gutiérrez, V.; Isidoro-García, L.; Dos santos-García, A.J. Magnetic $CoFe_2O_4$ Ferrite for Peroxymonosulfate Activation for Disinfection of Wastewater. *Chem. Eng. J.* **2020**, *398*, 125606. [CrossRef]
81. Peng, Y.; Tang, H.; Yao, B.; Gao, X.; Yang, X.; Zhou, Y. Activation of Peroxymonosulfate (PMS) by Spinel Ferrite and Their Composites in Degradation of Organic Pollutants: A Review. *Chem. Eng. J.* **2021**, *414*, 128800. [CrossRef]
82. Cai, C.; Liu, Y.; Xu, R.; Zhou, J.; Zhang, J.; Chen, Y.; Liu, L.; Zhang, L.; Kang, S.; Xie, X. Bicarbonate Enhanced Heterogeneous Activation of Peroxymonosulfate by Copper Ferrite Nanoparticles for the Efficient Degradation of Refractory Organic Contaminants in Water. *Chemosphere* **2023**, *312*, 137285. [CrossRef]
83. Chandel, M.; Ghosh, B.K.; Moitra, D.; Patra, M.K.; Vadera, S.R.; Ghosh, N.N. Synthesis of Various Ferrite (MFe_2O_4) Nanoparticles and Their Application as Efficient and Magnetically Separable Catalyst for Biginelli Reaction. *J. Nanosci. Nanotechnol.* **2018**, *18*, 2481–2492. [CrossRef]
84. Golshan, M.; Tian, N.; Mamba, G.; Kakavandi, B. Synergetic Photocatalytic Peroxymonosulfate Oxidation of Benzotriazole by Copper Ferrite Spinel: Factors and Mechanism Analysis. *Toxics* **2023**, *11*, 429. [CrossRef] [PubMed]
85. Niu, L.; Zhang, G.; Xian, G.; Ren, Z.; Wei, T.; Li, Q.; Zhang, Y.; Zou, Z. Tetracycline Degradation by Persulfate Activated with Magnetic γ-Fe_2O_3/CeO_2 Catalyst: Performance, Activation Mechanism and Degradation Pathway. *Sep. Purif. Technol.* **2021**, *259*, 118156. [CrossRef]
86. Deraz, N.M. Production and Characterization of Pure and Doped Copper Ferrite Nanoparticles. *J. Anal. Appl. Pyrolysis* **2008**, *82*, 212–222. [CrossRef]
87. Subha, A.; Shalini, M.G.; Sahu, B.N.; Rout, S.; Sahoo, S.C. Role of Surface Defects and Anisotropy Variation on Magnetic Properties of Copper Ferrite Nanoparticles Prepared by Co-Precipitation Method. *Mater. Chem. Phys.* **2022**, *286*, 126212. [CrossRef]
88. Ismael, M.; Wark, M. A Simple Sol–Gel Method for the Synthesis of Pt Co-Catalyzed Spinel-Type $CuFe_2O_4$ for Hydrogen Production; the Role of Crystallinity and Band Gap Energy. *Fuel* **2024**, *359*, 130429. [CrossRef]
89. Amulya, M.A.S.; Nagaswarupa, H.P.; Kumar, M.R.A.; Ravikumar, C.R.; Kusuma, K.B.; Prashantha, S.C. Evaluation of Bifunctional Applications of $CuFe_2O_4$ Nanoparticles Synthesized by a Sonochemical Method. *J. Phys. Chem. Solids* **2021**, *148*, 109756. [CrossRef]
90. Karakaş, Z.K. A Comprehensive Study on the Production and Photocatalytic Activity of Copper Ferrite Nanoparticles Synthesized by Microwave-Assisted Combustion Method as an Effective Photocatalyst. *J. Phys. Chem. Solids* **2022**, *170*, 110927. [CrossRef]
91. Cao, X.; Xiao, F.; Lyu, Z.; Xie, X.; Zhang, Z.; Dong, X.; Wang, J.; Lyu, X.; Zhang, Y.; Liang, Y. $CuFe_2O_4$ Supported on Montmorillonite to Activate Peroxymonosulfate for Efficient Ofloxacin Degradation. *J. Water Process Eng.* **2021**, *44*, 102359. [CrossRef]
92. Guan, Y.-H.; Ma, J.; Ren, Y.-M.; Liu, Y.-L.; Xiao, J.-Y.; Lin, L.; Zhang, C. Efficient Degradation of Atrazine by Magnetic Porous Copper Ferrite Catalyzed Peroxymonosulfate Oxidation via the Formation of Hydroxyl and Sulfate Radicals. *Water Res.* **2013**, *47*, 5431–5438. [CrossRef]
93. Zhao, J.; Xiao, P.; Han, S.; Zulhumar, M.; Wu, D. Preparation of Magnetic Copper Ferrite Nanoparticle as Peroxymonosulfate Activating Catalyst for Effective Degradation of Levofloxacin. *Water Sci. Technol.* **2022**, *85*, 645–663. [CrossRef] [PubMed]
94. Yu, S.; Zhang, Q.; Sun, X.; Chen, S.; Tang, J.; Zhu, J.-J.; Dang, Y. Doping Sb into $CuFe_2O_4$ Improved the Catalytic Performance in the Electrochemically Enhanced Homogeneous Peroxymonosulfate-Heterogeneous Catalytic System for the Degradation of Ciprofloxacin. *J. Environ. Chem. Eng.* **2022**, *10*, 108335. [CrossRef]

95. Feng, Y.; Wu, D.; Deng, Y.; Zhang, T.; Shih, K. Sulfate Radical-Mediated Degradation of Sulfadiazine by $CuFeO_2$ Rhombohedral Crystal-Catalyzed Peroxymonosulfate: Synergistic Effects and Mechanisms. *Environ. Sci. Technol.* **2016**, *50*, 3119–3127. [CrossRef] [PubMed]
96. Oh, W.-D.; Dong, Z.; Hu, Z.-T.; Lim, T.-T. A Novel Quasi-Cubic $CuFe_2O_4$–Fe_2O_3 Catalyst Prepared at Low Temperature for Enhanced Oxidation of Bisphenol A via Peroxymonosulfate Activation. *J. Mater. Chem. A Mater.* **2015**, *3*, 22208–22217. [CrossRef]
97. Zhao, X.; Wu, W.; Jing, G.; Zhou, Z. Activation of Sulfite Autoxidation with $CuFe_2O_4$ Prepared by MOF-Templated Method for Abatement of Organic Contaminants. *Environ. Pollut.* **2020**, *260*, 114038. [CrossRef]
98. Johnson, D.A. *Some Thermodynamic Aspects of Inorganic Chemistry*; Cambridge University Press: Cambridge, UK, 1982; ISBN 0521242045.
99. Moser, J.; Punchihewa, S.; Infelta, P.P.; Graetzel, M. Surface Complexation of Colloidal Semiconductors Strongly Enhances Interfacial Electron-Transfer Rates. *Langmuir* **1991**, *7*, 3012–3018. [CrossRef]
100. Popova, T.V.; Aksenova, N. V Complexes of Copper in Unstable Oxidation States. *Russ. J. Coord. Chem.* **2003**, *29*, 743–765. [CrossRef]
101. Mo, Q.; Zheng, H.; Sheng, G. A Heterogeneously Activated Peroxymonosulfate with a Co and Cu Codoped Bimetallic Metal-Organic Framework Efficiently Degrades Tetracycline in Water. *Mol. Catal.* **2024**, *553*, 113817. [CrossRef]
102. Guo, R.; Zhu, Y.; Cheng, X.; Li, J.; Crittenden, J.C. Efficient Degradation of Lomefloxacin by Co-Cu-LDH Activating Peroxymonosulfate Process: Optimization, Dynamics, Degradation Pathway and Mechanism. *J. Hazard. Mater.* **2020**, *399*, 122966. [CrossRef] [PubMed]
103. Sheikh Asadi, A.M.; Cichocki, Ł.; Atamaleki, A.; Hashemi, M.; Lutze, H.; Imran, M.; Kong, L.; Wang, C.; Boczkaj, G. Catalysts for Advanced Oxidation Processes: Deep Eutectic Solvents-Assisted Synthesis—A Review. *Water Resour. Ind.* **2024**, *31*, 100251. [CrossRef]
104. Fdez-Sanromán, A.; Rosales, E.; Pazos, M.; Sanroman, A. Metal–Organic Frameworks as Powerful Heterogeneous Catalysts in Advanced Oxidation Processes for Wastewater Treatment. *Appl. Sci.* **2022**, *12*, 8240. [CrossRef]
105. Chen, Y.; Zhang, Y.; Huang, Q.; Lin, X.; Zeb, A.; Wu, Y.; Xu, Z.; Xu, X. Recent Advances in Cu-Based Metal–Organic Frameworks and Their Derivatives for Battery Applications. *ACS Appl. Energy Mater.* **2022**, *5*, 7842–7873. [CrossRef]
106. Al-Wasidi, A.S.; AlMohisen, H.M.; Almehizia, A.A.; Naglah, A.M.; Tarek, M.; Said, G.E.; Khatab, T.K. Cu-Vit B3 MOF Solvothermal Preparation, Characterization and Evaluation as HIV-1 RNA Replication Inhibitor. *J. Mol. Struct.* **2024**, *1317*, 139120. [CrossRef]
107. Seo, Y.-K.; Hundal, G.; Jang, I.T.; Hwang, Y.K.; Jun, C.-H.; Chang, J.-S. Microwave Synthesis of Hybrid Inorganic–Organic Materials Including Porous $Cu_3(BTC)_2$ from Cu(II)-Trimesate Mixture. *Microporous Mesoporous Mater.* **2009**, *119*, 331–337. [CrossRef]
108. Campagnol, N.; Van Assche, T.R.C.; Li, M.; Stappers, L.; Dinca, M.; Denayer, J.F.M.; Binnemans, K.; De Vos, D.E.; Fransaer, J. On the Electrochemical Deposition of Metal-Organic Frameworks. *J. Mater. Chem. A Mater.* **2016**, *4*, 3914–3925. [CrossRef]
109. Li, Z.-Q.; Qiu, L.-G.; Xu, T.; Wu, Y.; Wang, W.; Wu, Z.-Y.; Jiang, X. Ultrasonic Synthesis of the Microporous Metal–Organic Framework $Cu_3(BTC)_2$ at Ambient Temperature and Pressure: An Efficient and Environmentally Friendly Method. *Mater. Lett.* **2009**, *63*, 78–80. [CrossRef]
110. Klimakow, M.; Klobes, P.; Rademann, K.; Emmerling, F. Characterization of Mechanochemically Synthesized MOFs. *Microporous Mesoporous Mater.* **2012**, *154*, 113–118. [CrossRef]
111. Xiang, Z.; Cao, D.; Shao, X.; Wang, W.; Zhang, J.; Wu, W. Facile Preparation of High-Capacity Hydrogen Storage Metal-Organic Frameworks: A Combination of Microwave-Assisted Solvothermal Synthesis and Supercritical Activation. *Chem. Eng. Sci.* **2010**, *65*, 3140–3146. [CrossRef]
112. Bai, Y.; Nie, G.; He, Y.; Li, C.; Wang, X.; Ye, L. Cu-MOF for Effectively Organic Pollutants Degradation and *E. coli* Inactivation via Catalytic Activation of Peroxymonosulfate. *J. Taiwan Inst. Chem. Eng.* **2022**, *132*, 104154. [CrossRef]
113. Quan, X.; Zhang, J.; Yin, L.; Tian, Y. Enhanced PMS Activation and NSAID Degradation Selectivity by Hydrophobic Microenvironment Regulation on Fe^{3+}@Cu-MOF. *Colloids Surf. A Physicochem. Eng. Asp.* **2024**, *695*, 134156. [CrossRef]
114. Zheng, H.; Zhou, Y.; Wang, D.; Zhu, M.; Sun, X.; Jiang, S.; Fan, Y.; Zhang, D.; Zhang, L. Surface-Functionalized PVDF Membranes by Facile Synthetic Cu-MOF-74 for Enhanced Contaminant Degradation and Antifouling Performance. *Colloids Surf. A Physicochem. Eng. Asp.* **2022**, *651*, 129640. [CrossRef]
115. Wu, Y.; Liang, G.; Li, W.-B.; Zhong, X.-F.; Zhang, Y.-Y.; Ye, J.-W.; Yang, T.; Mo, Z.-W.; Chen, X.-M. Boosting the Degradation of Antibiotics via Peroxymonosulfate Activation with a Cu-Based Metal–Organic Framework. *Chem. Sci.* **2024**, *15*, 9733–9741. [CrossRef]
116. Li, H.; Yang, Z.; Lu, S.; Su, L.; Wang, C.; Huang, J.; Zhou, J.; Tang, J.; Huang, M. Nano-Porous Bimetallic CuCo-MOF-74 with Coordinatively Unsaturated Metal Sites for Peroxymonosulfate Activation to Eliminate Organic Pollutants: Performance and Mechanism. *Chemosphere* **2021**, *273*, 129643. [CrossRef]
117. Wang, H.; Dai, Y.; Wang, Y.; Yin, L. One-Pot Solvothermal Synthesis of Cu–Fe-MOF for Efficiently Activating Peroxymonosulfate to Degrade Organic Pollutants in Water:Effect of Electron Shuttle. *Chemosphere* **2024**, *352*, 141333. [CrossRef]
118. Fdez-Sanromán, A.; Lomba-Fernández, B.; Pazos, M.; Rosales, E.; Sanromán, A. Peroxymonosulfate Activation by Different Synthesized CuFe-MOFs: Application for Dye, Drugs, and Pathogen Removal. *Catalysts* **2023**, *13*, 820. [CrossRef]
119. Zhu, Q.; Chen, L.; Zhu, T.; Gao, Z.; Wang, C.; Geng, R.; Bai, W.; Cao, Y.; Zhu, J. Contribution of $^1O_2$ in the Efficient Degradation of Organic Pollutants with $Cu^0/Cu_2O/CuO$@N–C Activated Peroxymonosulfate: A Case Study with Tetracycline. *Environ. Pollut.* **2024**, *342*, 123064. [CrossRef]

120. Ji, Y.; Li, W.; Cao, W.; Yang, Z.; Zheng, C.; Zhang, W. Effective Degradation of Organic Pollutants by CuFe@C Composite Derived from Bimetallic MOFs Synthesized through Stepwise Feeding Method. *J. Environ. Chem. Eng.* **2024**, *12*, 112792. [CrossRef]
121. Boumeriame, H.; Da Silva, E.S.; Cherevan, A.S.; Chafik, T.; Faria, J.L.; Eder, D. Layered Double Hydroxide (LDH)-Based Materials: A Mini-Review on Strategies to Improve the Performance for Photocatalytic Water Splitting. *J. Energy Chem.* **2022**, *64*, 406–431. [CrossRef]
122. Luo, L.; Wang, Y.; Zhu, M.; Cheng, X.; Zhang, X.; Meng, X.; Huang, X.; Hao, H. Co–Cu–Al Layered Double Oxides as Heterogeneous Catalyst for Enhanced Degradation of Organic Pollutants in Wastewater by Activating Peroxymonosulfate: Performance and Synergistic Effect. *Ind. Eng. Chem. Res.* **2019**, *58*, 8699–8711. [CrossRef]
123. Chiericatti, C.; Basilico, J.C.; Zapata Basilico, M.L.; Zamaro, J.M. Novel Application of HKUST-1 Metal–Organic Framework as Antifungal: Biological Tests and Physicochemical Characterizations. *Microporous Mesoporous Mater.* **2012**, *162*, 60–63. [CrossRef]
124. Giráldez, A.; Fdez-Sanromán, A.; Terrón, D.; Sanromán, M.A.; Pazos, M. Nanostructured Copper-Organic Frameworks for the Generation of Sulphate Radicals: Application in Wastewater Disinfection. *Environ. Sci. Pollut. Res.* **2023**. [CrossRef]
125. Li, H.; Xu, C.; Li, N.; Rao, T.; Zhou, Z.; Zhou, Q.; Wang, C.; Xu, S.; Tang, J. Synthesis of Bimetallic FeCu-MOF and Its Performance as Catalyst of Peroxymonosulfate for Degradation of Methylene Blue. *Materials* **2022**, *15*, 7252. [CrossRef] [PubMed]
126. Liu, X.; Zhou, J.; Liu, D.; Liu, S. Co Isomorphic Substitution for Cu-Based Metal Organic Framework Based on Electronic Structure Modulation Boosts Fenton-like Process. *Sep. Purif. Technol.* **2023**, *306*, 122526. [CrossRef]
127. Fdez-Sanromán, A.; Rosales, E.; Pazos, M.; Sanromán, A. One-Pot Synthesis of Bimetallic Fe–Cu Metal–Organic Frameworks Composite for the Elimination of Organic Pollutants via Peroxymonosulphate Activation. *Environ. Sci. Pollut. Res.* **2023**. [CrossRef] [PubMed]
128. Zhu, J.; Zhu, Z.; Zhang, H.; Lu, H.; Qiu, Y. Efficient Degradation of Organic Pollutants by Peroxymonosulfate Activated with MgCuFe-Layered Double Hydroxide. *RSC Adv.* **2019**, *9*, 2284–2291. [CrossRef] [PubMed]
129. Lu, H.; Sui, M.; Yuan, B.; Wang, J.; Lv, Y. Efficient Degradation of Nitrobenzene by Cu-Co-Fe-LDH Catalyzed Peroxymonosulfate to Produce Hydroxyl Radicals. *Chem. Eng. J.* **2019**, *357*, 140–149. [CrossRef]
130. Xie, M.; Liang, M.; Liu, C.; Xu, Z.; Yu, Y.; Xu, J.; You, S.; Wang, D.; Rad, S. Peroxymonosulfate Activation by CuMn-LDH for the Degradation of Bisphenol A: Effect, Mechanism, and Pathway. *Ecotoxicol. Environ. Saf.* **2024**, *270*, 115929. [CrossRef]
131. Guo, R.; Li, Y.; Chen, Y.; Liu, Y.; Niu, B.; Gou, J.; Cheng, X. Efficient Degradation of Sulfamethoxazole by CoCu LDH Composite Membrane Activating Peroxymonosulfate with Decreased Metal Ion Leaching. *Chem. Eng. J.* **2021**, *417*, 127887. [CrossRef]
132. Wu, L.; Jin, T.; Li, D.; Wang, L.; Sun, Y. Heterogeneous Activation of Permonosulfate by Biochar Supporting CuCoFe Layered Double Hydroxide for Rapid Degradation of Phenanthrene. *J. Environ. Chem. Eng.* **2023**, *11*, 110718. [CrossRef]
133. Dung, N.T.; Thao, V.D.; Huy, N.N. Decomposition of Glyphosate in Water by Peroxymonosulfate Activated with CuCoFe-LDH Material. *Vietnam. J. Chem.* **2021**, *59*, 813–822. [CrossRef]
134. Zhang, S.; Yan, Y.; Hu, W.; Fan, Y. Mesoporous CuO Prepared in a Natural Deep Eutectic Solvent Medium for Effective Photodegradation of Rhodamine B. *Molecules* **2023**, *28*, 5554. [CrossRef]
135. Patil, Y.A.; Shankarling, G.S. Deep Eutectic Solvent-Mediated, Energy-Efficient Synthesis of Copper Terephthalate Metal-Organic Framework and Its Application in Degradation of an Azo Dye. *Chem. Eng. J. Adv.* **2020**, *3*, 100032. [CrossRef]
136. Shahzad, A.; Jawad, A.; Ifthikar, J.; Chen, Z.; Chen, Z. The Hetero-Assembly of Reduced Graphene Oxide and Hydroxide Nanosheets as Superlattice Materials in PMS Activation. *Carbon* **2019**, *155*, 740–755. [CrossRef]
137. Shahzad, A.; Ali, J.; Ifthikar, J.; Aregay, G.G.; Zhu, J.; Chen, Z.; Chen, Z. Non-Radical PMS Activation by the Nanohybrid Material with Periodic Confinement of Reduced Graphene Oxide (RGO) and Cu Hydroxides. *J. Hazard. Mater.* **2020**, *392*, 122316. [CrossRef] [PubMed]
138. Smith, E.L.; Abbott, A.P.; Ryder, K.S. Deep Eutectic Solvents (DESs) and Their Applications. *Chem. Rev.* **2014**, *114*, 11060–11082. [CrossRef] [PubMed]
139. Álvarez, M.S.; Longo, M.A.; Rodríguez, A.; Deive, F.J. The Role of Deep Eutectic Solvents in Catalysis. A Vision on Their Contribution to Homogeneous, Heterogeneous and Electrocatalytic Processes. *J. Ind. Eng. Chem.* **2024**, *132*, 36–49. [CrossRef]
140. Abbott, A.P.; Capper, G.; Davies, D.L.; Munro, H.L.; Rasheed, R.K.; Tambyrajah, V. Preparation of Novel, Moisture-Stable, Lewis-Acidic Ionic Liquids Containing Quaternary Ammonium Salts with Functional Side Chains. *Chem. Commun.* **2001**, *1*, 2010–2011. [CrossRef]
141. Peng, Q.; Ye, L.; Wen, N.; Chen, H.; Zhu, Y.; Niu, H.; Tian, H.; Huang, D.; Huang, Y. Nitrogen Vacancy-Modified g-C_3N_4 Nanosheets Controlled by Deep Eutectic Solvents for Highly Efficient Photocatalytic Atrazine Degradation: Non-Radical Dominated Holes Oxidation. *Sep. Purif. Technol.* **2025**, *354*, 128879. [CrossRef]
142. Plaza-Mayoral, E.; Dalby, K.N.; Falsig, H.; Chorkendorff, I.; Sebastián-Pascual, P.; Escudero-Escribano, M. Preparation of Tunable Cu−Ag Nanostructures by Electrodeposition in a Deep Eutectic Solvent. *ChemElectroChem* **2024**, *11*, e202400094. [CrossRef]
143. Liang, C.; Huang, C.-F.; Mohanty, N.; Kurakalva, R.M. A Rapid Spectrophotometric Determination of Persulfate Anion in ISCO. *Chemosphere* **2008**, *73*, 1540–1543. [CrossRef] [PubMed]
144. Araújo, K.C.; Nóbrega, E.T.D.; Moreira, A.J.; Lemos, S.G.; Fragoso, W.D.; Pereira, E.C. Fast and Efficient Processes for Oxidation and Monitoring of Polycyclic Aromatic Hydrocarbons in Environmental Matrices. *Catal. Commun.* **2024**, *187*, 1068340. [CrossRef]
145. Moreira, A.J.; Borges, A.C.; De Souza, B.B.; Barbosa, L.R.; De Mendonça, V.R.; Freschi, C.D.; Freschi, G.P.G. Microwave Discharge Electrodeless Mercury Lamp (Hg-MDEL): An Energetic, Mechanistic and Kinetic Approach to the Degradation of Prozac. *J. Environ. Chem. Eng.* **2019**, *7*, 102916. [CrossRef]

146. Wang, L.; Lan, X.; Peng, W.; Wang, Z. Uncertainty and Misinterpretation over Identification, Quantification and Transformation of Reactive Species Generated in Catalytic Oxidation Processes: A Review. *J. Hazard. Mater.* **2021**, *408*, 124436. [CrossRef] [PubMed]
147. Li, X.; Jia, Y.; Zhou, M.; Su, X.; Sun, J. High-Efficiency Degradation of Organic Pollutants with Fe, N Co-Doped Biochar Catalysts via Persulfate Activation. *J. Hazard. Mater.* **2020**, *397*, 122764. [CrossRef]
148. Yang, Y.; Guo, C.; Zeng, Y.; Luo, Y.; Xu, J.; Wang, C. Peroxymonosulfate Activation by CuFe-Prussian Blue Analogues for the Degradation of Bisphenol S: Effect, Mechanism, and Pathway. *Chemosphere* **2023**, *331*, 138748. [CrossRef]
149. Xu, X.; Qin, J.; Wei, Y.; Ye, S.; Shen, J.; Yao, Y.; Ding, B.; Shu, Y.; He, G.; Chen, H. Heterogeneous Activation of Persulfate by $NiFe_{2-X}Co_xO_4$-RGO for Oxidative Degradation of Bisphenol A in Water. *Chem. Eng. J.* **2019**, *365*, 259–269. [CrossRef]
150. Liu, B.; Song, W.; Zhang, W.; Zhang, X.; Pan, S.; Wu, H.; Sun, Y.; Xu, Y. Fe_3O_4@CNT as a High-Effective and Steady Chainmail Catalyst for Tetracycline Degradation with Peroxydisulfate Activation: Performance and Mechanism. *Sep. Purif. Technol.* **2021**, *273*, 118705. [CrossRef]
151. Wang, Y.; Sun, H.; Ang, H.M.; Tadé, M.O.; Wang, S. Facile Synthesis of Hierarchically Structured Magnetic $MnO_2/ZnFe_2O_4$ Hybrid Materials and Their Performance in Heterogeneous Activation of Peroxymonosulfate. *ACS Appl. Mater. Interfaces* **2014**, *6*, 19914–19923. [CrossRef]
152. Nardi, G.; Manet, I.; Monti, S.; Miranda, M.A.; Lhiaubet-Vallet, V. Scope and Limitations of the TEMPO/EPR Method for Singlet Oxygen Detection: The Misleading Role of Electron Transfer. *Free Radic. Biol. Med.* **2014**, *77*, 64–70. [CrossRef]
153. Yun, E.-T.; Lee, J.H.; Kim, J.; Park, H.-D.; Lee, J. Identifying the Nonradical Mechanism in the Peroxymonosulfate Activation Process: Singlet Oxygenation versus Mediated Electron Transfer. *Environ. Sci. Technol.* **2018**, *52*, 7032–7042. [CrossRef] [PubMed]
154. Yao, Y.; Chen, H.; Lian, C.; Wei, F.; Zhang, D.; Wu, G.; Chen, B.; Wang, S. Fe, Co, Ni Nanocrystals Encapsulated in Nitrogen-Doped Carbon Nanotubes as Fenton-like Catalysts for Organic Pollutant Removal. *J. Hazard. Mater.* **2016**, *314*, 129–139. [CrossRef]
155. Shao, P.; Yin, X.; Yu, C.; Han, S.; Zhao, B.; Li, K.; Li, X.; Yang, Z.; Yuan, Z.; Shi, Q. Enhanced Activation of Peroxymonosulfate via Sulfate Radicals and Singlet Oxygen by $SrCo_xMn_{1-x}O_3$ Perovskites for the Degradation of Rhodamine B. *Processes* **2023**, *11*, 1279. [CrossRef]
156. Ghanbari, F.; Moradi, M. Application of Peroxymonosulfate and Its Activation Methods for Degradation of Environmental Organic Pollutants: Review. *Chem. Eng. J.* **2017**, *310*, 41–62. [CrossRef]
157. Zou, J.; Ma, J.; Zhang, J. Comment on Electrolytic Manipulation of Persulfate Reactivity by Iron Electrodes for TCE Degradation in Groundwater. *Environ. Sci. Technol.* **2014**, *48*, 4630–4631. [CrossRef] [PubMed]
158. Zhu, M.; Miao, J.; Duan, X.; Guan, D.; Zhong, Y.; Wang, S.; Zhou, W.; Shao, Z. Postsynthesis Growth of CoOOH Nanostructure on $SrCo_{0.6}Ti_{0.4}O_{3-\delta}$ Perovskite Surface for Enhanced Degradation of Aqueous Organic Contaminants. *ACS Sustain. Chem. Eng.* **2018**, *6*, 15737–15748. [CrossRef]
159. Liang, P.; Zhang, C.; Duan, X.; Sun, H.; Liu, S.; Tade, M.O.; Wang, S. N-Doped Graphene from Metal–Organic Frameworks for Catalytic Oxidation of p-Hydroxylbenzoic Acid: N-Functionality and Mechanism. *ACS Sustain. Chem. Eng.* **2017**, *5*, 2693–2701. [CrossRef]
160. Bokare, A.D.; Wonyong, C. Singlet-Oxygen Generation in Alkaline Periodate Solution. *Environ. Sci. Technol.* **2015**, *49*, 14392–14400. [CrossRef]
161. Haag, W.R.; Gassman, E. Singlet Oxygen in Surface Waters—Part I: Furfuryl Alcohol as a Trapping Agent. *Chemosphere* **1984**, *13*, 631–640. [CrossRef]
162. Yin, J.J.; Xia, Q.; Fu, P.P. UVA Photoirradiation of Anhydroretinol–Formation of Singlet Oxygen and Superoxide. *Toxicol. Ind. Health* **2007**, *23*, 625–631. [CrossRef] [PubMed]
163. Dong, C.; Bao, Y.; Sheng, T.; Yi, Q.; Zhu, Q.; Shen, B.; Xing, M.; Lo, I.M.C.; Zhang, J. Singlet Oxygen Triggered by Robust Bimetallic $MoFe/TiO_2$ Nanospheres of Highly Efficacy in Solar-Light-Driven Peroxymonosulfate Activation for Organic Pollutants Removal. *Appl. Catal. B* **2021**, *286*, 119930. [CrossRef]
164. Yang, P.; Li, S.; Xiaofu, L.; Xiaojing, A.; Liu, D.; Huang, W. Singlet Oxygen-Dominated Activation of Peroxymonosulfate by CuO/MXene Nanocomposites for Efficient Decontamination of Carbamazepine under High Salinity Conditions: Performance and Singlet Oxygen Evolution Mechanism. *Sep. Purif. Technol.* **2022**, *285*, 120288. [CrossRef]
165. Liang, C.; Su, H.-W. Identification of Sulfate and Hydroxyl Radicals in Thermally Activated Persulfate. *Ind. Eng. Chem. Res.* **2009**, *48*, 5558–5562. [CrossRef]
166. Zhao, J.; Chen, T.; Hou, C.; Huang, B.; Du, J.; Liu, N.; Zhou, X.; Zhang, Y. Efficient Activation of Peroxymonosulfate by Biochar-Loaded Zero-Valent Copper for Enrofloxacin Degradation: Singlet Oxygen-Dominated Oxidation Process. *Nanomaterials* **2022**, *12*, 2842. [CrossRef]
167. Teel, A.L.; Ahmad, M.; Watts, R.J. Persulfate Activation by Naturally Occurring Trace Minerals. *J. Hazard. Mater.* **2011**, *196*, 153–159. [CrossRef] [PubMed]
168. Huang, Y.-H.; Huang, Y.-F.; Huang, C.; Chen, C.-Y. Efficient Decolorization of Azo Dye Reactive Black B Involving Aromatic Fragment Degradation in Buffered Co^{2+}/PMS Oxidative Processes with a Ppb Level Dosage of Co^{2+}-Catalyst. *J. Hazard. Mater.* **2009**, *170*, 1110–1118. [CrossRef]
169. Sun, J.; Song, M.; Feng, J.; Pi, Y. Highly Efficient Degradation of Ofloxacin by UV/Oxone/Co^{2+} Oxidation Process. *Environ. Sci. Pollut. Res.* **2012**, *19*, 1536–1543. [CrossRef]
170. Mo, Y.; Xu, W.; Zhang, X.; Zhou, S. Enhanced Degradation of Rhodamine B through Peroxymonosulfate Activated by a Metal Oxide/Carbon Nitride Composite. *Water* **2022**, *14*, 2054. [CrossRef]

171. Shah, N.S.; Khan, J.A.; Sayed, M.; Khan, Z.U.H.; Ali, H.S.; Murtaza, B.; Khan, H.M.; Imran, M.; Muhammad, N. Hydroxyl and Sulfate Radical Mediated Degradation of Ciprofloxacin Using Nano Zerovalent Manganese Catalyzed $S_2O_8^{2-}$. *Chem. Eng. J.* **2019**, *356*, 199–209. [CrossRef]
172. Zhu, S.; Li, X.; Kang, J.; Duan, X.; Wang, S. Persulfate Activation on Crystallographic Manganese Oxides: Mechanism of Singlet Oxygen Evolution for Nonradical Selective Degradation of Aqueous Contaminants. *Environ. Sci. Technol.* **2018**, *53*, 307–315. [CrossRef] [PubMed]
173. Jing, K.; Li, R.; Wang, F.; Ping, C.; Lv, W. Sulfate Radical-Induced Transformation of Trimethoprim with $CuFe_2O_4$/MWCNTs as a Heterogeneous Catalyst of Peroxymonosulfate: Mechanisms and Reaction Pathways. *RSC Adv.* **2018**, *8*, 24787–24795.
174. Olmez-Hanci, T.; Arslan-Alaton, I. Comparison of Sulfate and Hydroxyl Radical Based Advanced Oxidation of Phenol. *Chem. Eng. J.* **2013**, *224*, 10–16. [CrossRef]
175. Lee, Y.; Lee, S.; Cui, M.; Ren, Y.; Park, B.; Ma, J.; Han, Z.; Khim, J. Activation of Peroxodisulfate and Peroxymonosulfate by Ultrasound with Different Frequencies: Impact on Ibuprofen Removal Efficient, Cost Estimation and Energy Analysis. *Chem. Eng. J.* **2021**, *413*, 127487. [CrossRef]
176. Zhang, H.; Xie, C.; Chen, L.; Duan, J.; Li, F.; Liu, W. Different Reaction Mechanisms of $SO^{4\bullet-}$ And•OH with Organic Compound Interpreted at Molecular Orbital Level in Co (II)/Peroxymonosulfate Catalytic Activation System. *Water Res.* **2023**, *229*, 119392. [CrossRef]
177. Avetta, P.; Pensato, A.; Minella, M.; Malandrino, M.; Maurino, V.; Minero, C.; Hanna, K.; Vione, D. Activation of Persulfate by Irradiated Magnetite: Implications for the Degradation of Phenol under Heterogeneous Photo-Fenton-like Conditions. *Environ. Sci. Technol.* **2015**, *49*, 1043–1050. [CrossRef]
178. Ma, Q.; Zhang, H.; Zhang, X.; Li, B.; Guo, R.; Cheng, Q.; Cheng, X. Synthesis of Magnetic CuO/$MnFe_2O_4$ Nanocompisite and Its High Activity for Degradation of Levofloxacin by Activation of Persulfate. *Chem. Eng. J.* **2019**, *360*, 848–860. [CrossRef]
179. Wang, X.; Ding, Y.; Dionysiou, D.D.; Liu, C.; Tong, Y.; Gao, J.; Fang, G.; Zhou, D. Efficient Activation of Peroxymonosulfate by Copper Sulfide for Diethyl Phthalate Degradation: Performance, Radical Generation and Mechanism. *Sci. Total Environ.* **2020**, *749*, 142387. [CrossRef]
180. Ma, W.; Wang, N.; Fan, Y.; Tong, T.; Han, X.; Du, Y. Non-Radical-Dominated Catalytic Degradation of Bisphenol A by ZIF-67 Derived Nitrogen-Doped Carbon Nanotubes Frameworks in the Presence of Peroxymonosulfate. *Chem. Eng. J.* **2018**, *336*, 721–731. [CrossRef]
181. Wang, Y.; Sun, H.; Ang, H.M.; Tadé, M.O.; Wang, S. Magnetic Fe_3O_4/Carbon Sphere/Cobalt Composites for Catalytic Oxidation of Phenol Solutions with Sulfate Radicals. *Chem. Eng. J.* **2014**, *245*, 1–9. [CrossRef]
182. Huang, B.-C.; Jiang, J.; Huang, G.-X.; Yu, H.-Q. Sludge Biochar-Based Catalysts for Improved Pollutant Degradation by Activating Peroxymonosulfate. *J. Mater. Chem. A Mater.* **2018**, *6*, 8978–8985. [CrossRef]
183. Fan, Y.; Ma, W.; He, J.; Du, Y. $CoMoO_4$ as a Novel Heterogeneous Catalyst of Peroxymonosulfate Activation for the Degradation of Organic Dyes. *RSC Adv.* **2017**, *7*, 36193–36200. [CrossRef]
184. Yu, B.; Li, Z.; Zhang, S. Zero-Valent Copper-Mediated Peroxymonosulfate Activation for Efficient Degradation of Azo Dye Orange G. *Catalysts* **2022**, *12*, 700. [CrossRef]
185. Oh, W.-D.; Veksha, A.; Chen, X.; Adnan, R.; Lim, J.-W.; Leong, K.-H.; Lim, T.-T. Catalytically Active Nitrogen-Doped Porous Carbon Derived from Biowastes for Organics Removal via Peroxymonosulfate Activation. *Chem. Eng. J.* **2019**, *374*, 947–957. [CrossRef]
186. Wang, Z.; Yuan, R.; Guo, Y.; Xu, L.; Liu, J. Effects of Chloride Ions on Bleaching of Azo Dyes by Co^{2+}/Oxone Regent: Kinetic Analysis. *J. Hazard. Mater.* **2011**, *190*, 1083–1087. [CrossRef]
187. Wang, P.; Yang, S.; Shan, L.; Niu, R.; Shao, X. Involvements of Chloride Ion in Decolorization of Acid Orange 7 by Activated Peroxydisulfate or Peroxymonosulfate Oxidation. *J. Environ. Sci.* **2011**, *23*, 1799–1807. [CrossRef]
188. Yuan, R.; Ramjaun, S.N.; Wang, Z.; Liu, J. Effects of Chloride Ion on Degradation of Acid Orange 7 by Sulfate Radical-Based Advanced Oxidation Process: Implications for Formation of Chlorinated Aromatic Compounds. *J. Hazard. Mater.* **2011**, *196*, 173–179. [CrossRef]
189. Chan, K.H.; Chu, W. Degradation of Atrazine by Cobalt-Mediated Activation of Peroxymonosulfate: Different Cobalt Counteranions in Homogenous Process and Cobalt Oxide Catalysts in Photolytic Heterogeneous Process. *Water Res.* **2009**, *43*, 2513–2521. [CrossRef] [PubMed]
190. Zhu, S.; Huang, X.; Ma, F.; Wang, L.; Duan, X.; Wang, S. Catalytic Removal of Aqueous Contaminants on N-Doped Graphitic Biochars: Inherent Roles of Adsorption and Nonradical Mechanisms. *Environ. Sci. Technol.* **2018**, *52*, 8649–8658. [CrossRef]
191. Faheem; Du, J.; Kim, S.H.; Hassan, M.A.; Irshad, S.; Bao, J. Application of Biochar in Advanced Oxidation Processes: Supportive, Adsorptive, and Catalytic Role. *Environ. Sci. Pollut. Res.* **2020**, *27*, 37286–37312. [CrossRef]
192. Xiao, S.; Cheng, M.; Zhong, H.; Liu, Z.; Liu, Y.; Yang, X.; Liang, Q. Iron-Mediated Activation of Persulfate and Peroxymonosulfate in Both Homogeneous and Heterogeneous Ways: A Review. *Chem. Eng. J.* **2020**, *384*, 123265. [CrossRef]
193. Duan, X.; Ao, Z.; Zhou, L.; Sun, H.; Wang, G.; Wang, S. Occurrence of Radical and Nonradical Pathways from Carbocatalysts for Aqueous and Nonaqueous Catalytic Oxidation. *Appl. Catal. B* **2016**, *188*, 98–105. [CrossRef]
194. Jiang, M.; Lu, J.; Ji, Y.; Kong, D. Bicarbonate-Activated Persulfate Oxidation of Acetaminophen. *Water Res.* **2017**, *116*, 324–331. [CrossRef] [PubMed]

195. Du, W.; Zhang, Q.; Shang, Y.; Wang, W.; Li, Q.; Yue, Q.; Gao, B.; Xu, X. Sulfate Saturated Biosorbent-Derived Co-S@ NC Nanoarchitecture as an Efficient Catalyst for Peroxymonosulfate Activation. *Appl. Catal. B* **2020**, *262*, 118302. [CrossRef]
196. Ye, S.; Zeng, G.; Tan, X.; Wu, H.; Liang, J.; Song, B.; Tang, N.; Zhang, P.; Yang, Y.; Chen, Q.; et al. Nitrogen-Doped Biochar Fiber with Graphitization from Boehmeria Nivea for Promoted Peroxymonosulfate Activation and Non-Radical Degradation Pathways with Enhancing Electron Transfer. *Appl. Catal. B* **2020**, *269*, 118850. [CrossRef]
197. Ji, Y.; Dong, C.; Kong, D.; Lu, J. New Insights into Atrazine Degradation by Cobalt Catalyzed Peroxymonosulfate Oxidation: Kinetics, Reaction Products and Transformation Mechanisms. *J. Hazard. Mater.* **2015**, *285*, 491–500. [CrossRef]
198. Drosos, M.; Ren, M.; Frimmel, F.H. The Effect of NOM to TiO_2: Interactions and Photocatalytic Behavior. *Appl. Catal. B* **2015**, *165*, 328–334. [CrossRef]
199. He, X.; de la Cruz, A.A.; O'Shea, K.E.; Dionysiou, D.D. Kinetics and Mechanisms of Cylindrospermopsin Destruction by Sulfate Radical-Based Advanced Oxidation Processes. *Water Res.* **2014**, *63*, 168–178. [CrossRef]
200. Nagar, N.; Devra, V. Activation of Peroxodisulfate and Peroxomonosulfate by Green Synthesized Copper Nanoparticles for Methyl Orange Degradation: A Kinetic Study. *J. Environ. Chem. Eng.* **2017**, *5*, 5793–5800. [CrossRef]
201. Guo, R.; Chen, Y.; Nengzi, L.; Meng, L.; Song, Q.; Gou, J.; Cheng, X. In Situ Preparation of Carbon-Based Cu-Fe Oxide Nanoparticles from CuFe Prussian Blue Analogues for the Photo-Assisted Heterogeneous Peroxymonosulfate Activation Process to Remove Lomefloxacin. *Chem. Eng. J.* **2020**, *398*, 125556. [CrossRef]
202. Chen, J.; Rasool, R.T.; Ashraf, G.A.; Guo, H. The Stimulation of Peroxymonosulfate via Novel $Co_{0.5}Cu_{0.5}Fe_2O_4$ Heterogeneous Photocatalyst in Aqueous Solution for Organic Contaminants Removal. *Mater. Sci. Semicond. Process* **2023**, *157*, 107321. [CrossRef]
203. Jaafarzadeh, N.; Ghanbari, F.; Ahmadi, M. Efficient Degradation of 2,4-Dichlorophenoxyacetic Acid by Peroxymonosulfate/Magnetic Copper Ferrite Nanoparticles/Ozone: A Novel Combination of Advanced Oxidation Processes. *Chem. Eng. J.* **2017**, *320*, 436–447. [CrossRef]
204. Yang, J.; Li, Y.; Yang, Z.; Shih, K.; Ying, G.-G.; Feng, Y. Activation of Ozone by Peroxymonosulfate for Selective Degradation of 1,4-Dioxane: Limited Water Matrices Effects. *J. Hazard. Mater.* **2022**, *436*, 129223. [CrossRef]
205. Feizi, R.; Ahmad, M.; Jorfi, S.; Ghanbari, F. Sunset Yellow Degradation by Ultrasound/Peroxymonosulfate/$CuFe_2O_4$: Influential Factors and Degradation Processes. *Korean J. Chem. Eng.* **2019**, *36*, 886–893. [CrossRef]
206. Liu, X.; Huang, F.; Yu, Y.; Zhao, P.; Zhou, Y.; He, Y.; Xu, Y.; Zhang, Y. Ofloxacin Degradation over Cu–Ce Tyre Carbon Catalysts by the Microwave Assisted Persulfate Process. *Appl. Catal. B* **2019**, *253*, 149–159. [CrossRef]
207. Mahamuni, N.N.; Adewuyi, Y.G. Advanced Oxidation Processes (AOPs) Involving Ultrasound for Waste Water Treatment: A Review with Emphasis on Cost Estimation. *Ultrason. Sonochem* **2010**, *17*, 990–1003. [CrossRef] [PubMed]
208. Guan, Y.-H.; Ma, J.; Li, X.-C.; Fang, J.-Y.; Chen, L.-W. Influence of PH on the Formation of Sulfate and Hydroxyl Radicals in the UV/Peroxymonosulfate System. *Environ. Sci. Technol.* **2011**, *45*, 9308–9314. [CrossRef] [PubMed]
209. Li, Z.; Liu, D.; Zhao, Y.; Li, S.; Wei, X.; Meng, F.; Huang, W.; Lei, Z. Singlet Oxygen Dominated Peroxymonosulfate Activation by CuO-CeO_2 for Organic Pollutants Degradation: Performance and Mechanism. *Chemosphere* **2019**, *233*, 549–558. [CrossRef] [PubMed]
210. Sui, C.; Nie, Z.; Liu, H.; Boczkaj, G.; Liu, W.; Kong, L.; Zhan, J. Singlet Oxygen-Dominated Peroxymonosulfate Activation by Layered Crednerite for Organic Pollutants Degradation in High Salinity Wastewater. *J. Environ. Sci.* **2024**, *135*, 86–96. [CrossRef]
211. Wei, Y.; Miao, J.; Ge, J.; Lang, J.; Yu, C.; Zhang, L.; Alvarez, P.J.J.; Long, M. Ultrahigh Peroxymonosulfate Utilization Efficiency over CuO Nanosheets via Heterogeneous Cu (III) Formation and Preferential Electron Transfer during Degradation of Phenols. *Environ. Sci. Technol.* **2022**, *56*, 8984–8992. [CrossRef]
212. Pan, J.; Gao, B.; Duan, P.; Guo, K.; Akram, M.; Xu, X.; Yue, Q.; Gao, Y. Improving Peroxymonosulfate Activation by Copper Ion-Saturated Adsorbent-Based Single Atom Catalysts for the Degradation of Organic Contaminants: Electron-Transfer Mechanism and the Key Role of Cu Single Atoms. *J. Mater. Chem. A Mater.* **2021**, *9*, 11604–11613. [CrossRef]
213. Shang, Y.; Chen, C.; Zhang, P.; Yue, Q.; Li, Y.; Gao, B.; Xu, X. Removal of Sulfamethoxazole from Water via Activation of Persulfate by Fe_3C@NCNTs Including Mechanism of Radical and Nonradical Process. *Chem. Eng. J.* **2019**, *375*, 122004. [CrossRef]
214. Liu, T.; Wu, K.; Wang, M.; Jing, C.; Chen, Y.; Yang, S.; Jin, P. Performance and Mechanisms of Sulfadiazine Removal Using Persulfate Activated by Fe_3O_4@CuOx Hollow Spheres. *Chemosphere* **2021**, *262*, 127845. [CrossRef] [PubMed]
215. Dung, N.T.; Trang, T.T.; Thao, V.D.; Thu, T.V.; Tung, N.Q.; Huy, N.N. Enhanced Degradation of Organic Dyes by Peroxymonosulfate with Fe_3O_4-$CoCO_3$/RGO Hybrid Activation: A Comprehensive Study. *J. Taiwan Inst. Chem. Eng.* **2022**, *133*, 104279. [CrossRef]
216. Tian, W.; Zhang, H.; Qian, Z.; Ouyang, T.; Sun, H.; Qin, J.; Tadé, M.O.; Wang, S. Bread-Making Synthesis of Hierarchically Co@C Nanoarchitecture in Heteroatom Doped Porous Carbons for Oxidative Degradation of Emerging Contaminants. *Appl. Catal. B* **2018**, *225*, 76–83. [CrossRef]
217. Duan, X.; Sun, H.; Shao, Z.; Wang, S. Nonradical Reactions in Environmental Remediation Processes: Uncertainty and Challenges. *Appl. Catal. B* **2018**, *224*, 973–982. [CrossRef]
218. Song, H.; Liu, Z.; Guan, Z.; Yang, F.; Xia, D.; Li, D. Efficient Persulfate Non-Radical Activation of Electron-Rich Copper Active Sites Induced by Oxygen on Graphitic Carbon Nitride. *Sci. Total Environ.* **2021**, *762*, 143127. [CrossRef]
219. Pang, Y.; Luo, K.; Tang, L.; Li, X.; Yu, J.; Guo, J.; Liu, Y.; Zhang, Z.; Yue, R.; Li, L. Carbon-Based Magnetic Nanocomposite as Catalyst for Persulfate Activation: A Critical Review. *Environ. Sci. Pollut. Res.* **2019**, *26*, 32764–32776. [CrossRef]

220. Yun, E.-T.; Yoo, H.-Y.; Bae, H.; Kim, H.-I.; Lee, J. Exploring the Role of Persulfate in the Activation Process: Radical Precursor versus Electron Acceptor. *Environ. Sci. Technol.* **2017**, *51*, 10090–10099. [CrossRef]
221. Wang, G.; An, W.; Zhang, Y.; Liu, Z.; Yang, S.; Jin, P.; Ding, D. Mesoporous Carbon Framework Supported Cu-Fe Oxides as Efficient Peroxymonosulfate Catalyst for Sustained Water Remediation. *Chem. Eng. J.* **2022**, *430*, 133060. [CrossRef]
222. Tian, M.; Ren, X.; Ding, S.; Fu, N.; Wei, Y.; Yang, Z.; Yao, X. Effective Degradation of Phenol by Activating PMS with Bimetallic Mo and Ni Co-Doped g C_3N_4 Composite Catalyst: A Fenton-like Degradation Process Promoted by Non-Free Radical $^1O_2$. *Environ. Res.* **2024**, *243*, 117848. [CrossRef] [PubMed]
223. Yang, Z.; Ren, X.; Ding, S.; Fan, X.; Lu, Z.; Fu, N.; Tian, M. Modulation of Morphology and Phase of Magnetically Separable 1T-WS_2/$CuFe_2O_4$ Heterojunctions for Acceleration of Peroxymonosulfate Decomposition for Rapid Degradation of Phenol. *Sep. Purif. Technol.* **2024**, *348*, 127635. [CrossRef]
224. Wang, Y.; Wang, S.; Liu, Y.; Wang, J. Visible Light-Enhanced Interface Interaction for PMS Activation towards the Removal of Emerging Organic Pollutants: Performance, Mechanism and Toxicity. *Sep. Purif. Technol.* **2025**, *354*, 128741. [CrossRef]
225. Zhang, X.; Bai, T.; Chen, R.; Zheng, S.; Yin, J.; Qi, G.; Li, X.; Zheng, H.; Sun, Y. Cobalt Oxides Grown In-Situ on Carbon Nitride Nanosheets for Efficient Peroxymonosulfate Activation and Organic Contaminants Degradation: Performance, Mechanism, and Application Study. *Sep. Purif. Technol.* **2025**, *353*, 128646. [CrossRef]
226. Sun, Q.; Hu, X.; Wang, H.; Liu, H.; Lin, Y.; Zhang, J.; Dong, X.; Sheng, J. Interfacial Engineering and Vacancy Design of Quasi-2D NiCoAl-LDH/Kaolin Hybrid for Activating Peroxymonosulfate to Boost Degradation of Antibiotics. *Sep. Purif. Technol.* **2025**, *354*, 128674. [CrossRef]
227. Ma, Y.; Meng, Y.; Wang, Z.; Xin, Y.; Lv, X.; Li, Q.; Wang, H.; Xie, H.; Zhang, Z. In-Situ Construction of Mesoporous $CuCo_2O_4$ Decorated CNTs Networks as a Long-Lasting Peroxymonosulfate Activator for Rapid Removal of Aqueous Micropollutants. *Chem. Eng. J.* **2023**, *476*, 146694. [CrossRef]
228. Brillas, E.; Peralta-Hernández, J.M. Antibiotic Removal from Synthetic and Real Aqueous Matrices by Peroxymonosulfate-Based Advanced Oxidation Processes. A Review of Recent Development. *Chemosphere* **2024**, *351*, 141153. [CrossRef] [PubMed]
229. Derbalah, A.; Sakugawa, H. Sulfate Radical-Based Advanced Oxidation Technology to Remove Pesticides from Water A Review of the Most Recent Technologies. *Int. J. Environ. Res.* **2024**, *18*, 11. [CrossRef]
230. Chen, K.; Zhou, L.; Xu, W.; Hu, Z.; Jia, M.; Liu, L. A Novel Way of Activating Peroxysulfate by Zero-Valent Copper and Ferroferric Oxide Co-Modified Biochar to Remove Bisphenol A in Aqueous Solution: Performance, Mechanism and Potential Toxicity. *Appl. Catal. A Gen.* **2022**, *636*, 118575. [CrossRef]
231. Li, H.; Su, L.; Zheng, J.; Lu, S.; Yang, Z.; Wang, C.; Xu, S.; Zhou, Q.; Tang, J.; Huang, M.; et al. MOFs Derived Carbon Supporting CuCo Nanospheres as Efficient Catalysts of Peroxymonosulfate for Rapid Removal of Organic Pollutant. *Chem. Eng. J.* **2023**, *451*, 139114. [CrossRef]
232. Liu, X.; Pei, Y.; Cao, M.; Yang, H.; Li, Y. Magnetic $CuFe_2O_4$ Nanoparticles Anchored on N-Doped Carbon for Activated Peroxymonosulfate Removal of Oxytetracycline from Water: Radical and Non-Radical Pathways. *Chemosphere* **2023**, *334*, 139025. [CrossRef] [PubMed]
233. Li, J.; Cheng, X.; Zhang, H.; Gou, J.; Zhang, X.; Wu, D.; Dionysiou, D.D. Insights into Performance and Mechanism of ZnO/$CuCo_2O_4$ Composite as Heterogeneous Photoactivator of Peroxymonosulfate for Enrofloxacin Degradation. *J. Hazard. Mater.* **2023**, *448*, 130946. [CrossRef] [PubMed]
234. Yan, J.; Li, J.; Peng, J.; Zhang, H.; Zhang, Y.; Lai, B. Efficient Degradation of Sulfamethoxazole by the CuO@Al_2O_3 (EPC) Coupled PMS System: Optimization, Degradation Pathways and Toxicity Evaluation. *Chem. Eng. J.* **2019**, *359*, 1097–1110. [CrossRef]
235. Huang, Y.; Li, X.; Zhang, C.; Dai, M.; Zhang, Z.; Xi, Y.; Quan, B.; Lu, S.; Liu, Y. Degrading Arsanilic Acid and Adsorbing the Released Inorganic Arsenic Simultaneously in Aqueous Media with $CuFe_2O_4$ Activating Peroxymonosulfate System: Factors, Performance, and Mechanism. *Chem. Eng. J.* **2021**, *424*, 128537. [CrossRef]